UNIVERSITY OF CALGARY

The role of protein phosphatase 4 in regulating microtubule severing in *C. elegans*

by

Xue Han

A THESIS

SUBMITTED TO THE FACULTY OF GRADUATE STUDIES

IN PARTIAL FULFILMENT OF THE REQUIREMENTS FOR THE

DEGREE OF MASTER OF SCIENCE

BIOCHEMISTRY AND MOLECULAR BIOLOGY

CALGARY, ALBERTA

August 2007

Abstract

mei-1 encodes the *C. elegans* "katanin" microtubule-severing protein, which is required during meiosis to regulate the shape and dynamics of meiotic spindles but MEI-1 must be degraded before the first mitosis. Degradation of post-meiotic MEI-1 is carried out by MEL-26/CUL-3 ubiquitin ligase, MBK-2 kinase and APC. My thesis focused on the major question of whether there are any other mechanisms to regulate MEI-1. The regulatory subunit of PP4, *ppfr-1* was previously identified as a suppressor of a *mei-1(gf)* allele that is refractory to degradation by MEL-26. I found that RNAi to three PP4 subunits, including PPH-4.1, PPFR-1 and PPFR-3 suppressed lethality of post-meiotic MEI-1. This suggests that PP4(+) normally activates MEI-1, and so loss of PP4 decreases ectopic MEI-1(gf) activity. Reducing PP4 in *mei-1(gf)* did not change protein level of post-meiotic MEI-1. It is quite likely that PP4 regulates MEI-1 activity via direct binding, to remove an inhibitory phosphate.

Acknowledgements

I would like to thank my supervisor, Dr. Paul Mains, for his patient guidance, support and encouragement. Thanks also to my committee members, Dr. Jim McGhee and Dr. Sarah Childs for their great suggestions and advice on my project, and to Dr. Manfred Lohka for serving as my external examiner.

Many thanks to past and present members of the University of Calgary Worm Research Group for sharing ideas and techniques. Thanks to Dr. Jim McGhee, Chenggang Lu, Jacque-Lynne Johnson, and Barbara Goszczynski for their patient guidance and help in my first year in the lab. Thanks to Christopher Vanneste, Eko Raharjo, Jingjing Luo, Jie Yan, Dong Hu and Bhaskar Gavinolla for friendship. Finally, thanks to my family, Mom, Dad and my fiancé Xiao Li, for their understanding and support.

Table of Contents

List of Tables

List of Figures and Illustrations

List of Symbols, Abbreviations and Nomenclature

Symbol	Definition
AAA	ATPase associated with various cellular activities
APC	anaphase promoting complex
A-P	anterior-posterior
bp	base pair
DIC	differential interference contrast
cM	centimorgans
DMP	dimethylpimelimidate
dsRNA	double stranded RNA
emb	abnormal embryogenesis
gf	gain-of-function
HB	homogenization buffer
hrs	hours
IP	immunoprecipitation
kDa	kilodalton
lf	loss-of-function
MALDI	Matrix-Assisted Laser Desorption/Ionization
lin	lineage defective
MAPs	microtubule-associated proteins
MAT	metaphase-anaphase transition
mbk	mini-brain kinase
mei	meiosis defective
mel	maternal effect lethal
MTs	microtubules
MTOC	microtubule organizing centres
NEBD	nuclear envelope break down
NHS	N-hydroxysuccinimide
PAGE	polyacrylamide gel electrophoresis
PBS	phosphate buffered saline
plk	polo-like kinase
PP4	Protein Phosphatase 4
ppfr	protein phosphatase four regulatory subunit
RNAi	RNA interference
SDS	sodium dodecyl sulfate
tba	tubulin alpha
tbg	tubulin gamma
ts	temperature sensitive
unc	uncoordinated
Y2H	yeast-2-hybrid
zyg	zygotic defective

Chapter One: Introduction

1.1 Mitosis and meiosis in *C. elegans.*

Sexual reproduction of eukaryotic organisms requires two distinct types of cell divisions, meiosis and mitosis. Meiosis is the process in which homologous chromosomes pair, recombine and then segregate to daughter cells to generate haploid gametes. Female meiosis usually arrests at a specific meiotic stage, which differs between organisms, until fertilization. For example, the *C. elegans* oocyte arrests at diakinesis of meiosis I (Albertson 1984). After fertilization, the oocyte quickly completes two rounds of division without an intervening period of DNA replication to generate one haploid female pronucleus and two polar bodies. At the end of meiosis, the female and male pronuclei migrate toward each other and fuse in the middle of the embryo and mitotic divisions immediately begin. In contrast to meiosis, during mitosis chromosome sets are maintained so that each daughter cell has an identical genome compared to the parent cell.

Meiosis differs from mitosis not only in the behaviour of chromosomes but also in the major structure of its tubulin cytoskeleton, the spindle apparatus. Like other animals, the *C. elegans* meiotic spindle is relatively small, and it is localized to the anterior cortex of the embryos (Figure 1). Restriction of the spindle length and cortical localization are believed to be important for unequal meiotic divisions, by which the non-viable polar bodies are discarded while most cytoplasm remains. In contrast to the meiotic spindle, the first mitotic spindle is large and fills the cell. It is positioned along the A-P axis, slightly posterior of the centre of the embryo (Figure 1). The distinct structures of the meiotic and

mitotic spindles reflect differences in organization of the spindle backbone components, namely microtubules (MTs).

MTs are polymers of a heterodimer composed of α- and β-tubulin monomers. Tubulin heterodimer subunits join to one another in an end-to-end manner to form a linear protofilament (Amos and Klug, 1974). Eleven protofilaments associate side by side to form the MT lattice in most *C. elegans* cells, except in the touch receptor neurons where there are 15 (Chalfie and Thomson, 1982). In most eukaryotes, MTs are composed of 13 protofilaments. MTs are polarized with a fast growing "plus" end and a slow growing "minus" end (Allen and Borisy, 1974). The stability of microtubules is regulated via GTP-dependent polymerization/depolymerization at the plus end as well as interactions between MTs and microtubule-associated proteins (MAPs).

In *C. elegans* and many other animals, formation of oocyte meiotic spindles is independent of centrosomes (Schatten, 1994). These so called acentrosomal spindles are assembled by an 'inside-out' mechanism, in which microtubules are nucleated from chromatin and further assembled into a bipolar meiotic spindle by motor proteins (Heald *et al.*, 1999). In contrast to the meiotic spindles, the mitotic spindles are organized by a pair of centrosomes, which come in with the sperm and function as MT organizing centres (MTOC) to nucleate microtubules. During mitosis, MT nucleation at centrosomes is catalyzed by γ-tubulin ring complexes (γ-TURCs) (Aldaz *et al.*, 2005). Most of the nucleated MTs are incorporated into the mitotic spindle structures by contacting chromosomes or spanning the regions between the poles while others interact with the cell cortex to position the spindle.

Thus, meiotic and mitotic spindles show dramatic differences not only in their localization and morphology, but also in the way they are assembled. Gene products unique to one or the other division must therefore be carefully regulated. This problem is particularly acute in *C. elegans* where the transition from meiosis to mitosis is completed within 10 minutes (Kemphues 1986, McCarter 1999). My work focuses on a phosphatase that appears to be regulating one such meiotic-specific component.

1.2 The MEI-1/MEI-2 microtubule-severing complex.

Maternal-effect embryonic lethal mutations in the *C. elegans mei-1*(meiosis defective) and *mei-2* genes have defects in the transition from meiosis to mitosis. The first class of mutations has meiosis failure but normal mitosis, indicating essential functions of these genes only during meiosis. These mutations include loss-of-function (*lf*) alleles of *mei-1* and *mei-2* (Mains *et al*., 1990ab, Clandinin and Mains, 1993). A second group of mutations instead disrupts the first mitotic divisions but has normal meiotic divisions. This group includes the gain-of-function (*gf*) alleles of *mei-1*, *gf* and *lf* alleles of *mel-26* (maternal effect lethal) (Mains *et al*, 1990b, Dow *et al.*, 1998), *lf* alleles of *zyg-9* (zygote defective, Kemphues *et al*., 1986, Mains *et al*., 1990b, Matthews *et al*., 1998) and *lf* mutations of *mbk-2* (mini-brain kinase-2) (Ming Pang *et al.*, 2004, Quintin *et al.*, 2003, Pellettieri *et al.*, 2003). Mutations in the second group have characteristic mitotic spindle defects, with the first mitotic spindle being not only smaller and more posteriorly located compared to wild type, but also oriented in a dorsal-ventral direction instead of the normal anterior-posterior direction (Figure 2). Except for the case of *zyg-9*, these mutant phenotypes reflect the improper regulation of components specific for the meiotic divisions during the subsequent mitosis, namely MEI-1 and MEI-2. In these

mutants, instead of being eliminated by post-meiotic inactivation and/or degradation as in wild-type embryos, *mei-1* gene product persists into mitotic spindles, resulting in mitosis failure (Figure 2).

Sequence analysis has shown that *mei-1* belongs to the AAA (ATPase Associated with various cellular Activities) gene family and is a homologue of the p60 subunit of the sea urchin MT-severing enzyme, katanin (Mains *et al*., 1990b and Srayko *et al*., 2000). Katanin is a heterooligomeric protein, including the p60 subunit with ATP-dependent MT-severing activity and the p80 subunit, which targets p60 to its substrates (McNally and Vale, 1993, Hartman *et al.,* 1998). Like in the sea urchin, the *C. elegans* MT-severing enzyme is composed of two subunits, the p60 homologue MEI-1 and the p80 homologue MEI-2. In wild-type worm embryos, MEI-1 and MEI-2 co-localize to the meiotic spindles and localization of one protein depends on the other (Srayko *et al*., 2000). Furthermore, co-expression of both proteins in Hela cells cause interphase MTs to disassemble (Srayko *et al*., 2000) and bacterially-expressed MEI-1 and MEI-2 can sever MTs *in vitro* (McNally *et al*., 2006). All of these findings favour the model that, similar to katanin in other organisms, *C. elegans* MEI-1 and MEI-2 form a complex *in vivo* to sever MTs. This model is further supported by the following studies linking MT-severing activity to the mutant phenotypes. Treatment of embryos with the MT depolymerising drug nocodazole has the same defect as ectopic MEI-1 expression (Strome and Wood, 1983; Hyman and White, 1987). More recently, MT fragmentation was visualized in wild-type but not in *mei-1(null)* spindles by using electron microscopy, confirming MEI-1 MT-severing activity *in vivo* (Srayko *et al.*, 2006).

Although the role of MT-severing by katanin is not yet fully understood, one possible explanation is that it is a mechanism to generate lots of short MT arrays that facilitate nucleation and assembly of the meiotic spindles in the absence of a traditional MTOC (Srayko *et al.*, 2006). Indeed, γ-tubulin dependent MT nucleation acts redundantly with katanin mediated MT-severing to increase MT numbers during meiosis (McNally *et al*., 2006). After spindle assembly, katanin has a role in the characteristic shortening of the *C. elegans* meiotic spindle that occurs during anaphase I and II. Spindle shortening can also be seen in nocodazole treated mammalian fibroblasts, and this also requires katanin (McNally *et al*., 2006).

To summarize, in *C. elegans,* the MEI-1/MEI-2 katanin enzyme exerts MT-severing activity, which is required during meiosis but which must be inactivated before mitosis. In the following paragraph, I will discuss pathways involved in post-meiotic degradation/inactivation of MEI-1.

1.3 MEI-1 degradation pathways.

mei-1 and *mei-2* are required for meiosis but must be eliminated efficiently during the transition to mitosis. The rapid turnover of MEI-1 resides in the PEST motif (a region rich in proline, glutamic acid, serine, and threonine) (Rogers *et al*., 1986), which serves as a tag for protein degradation (Rechsteiner and Rogers, 1996, Furukawa *et al.*, 2003, Pintard *et al.*, 2003, Xu *et al.*, 2003). Disruption of the PEST motif in the *mei-1(gf)* allele results in failure to eliminate MEI-1. As a result, ectopic MEI-1 persists into mitosis and causes defects in mitotic spindle assembly (Clark-Maguire and Mains, 1994b).

MEI-1 degradation requires not only the PEST motif but also an ubiquitin-ligase complex that includes CUL-3 and the BTB protein MEL-26 (Clark-Maguire and Mains,

1994b, Dow and Mains, 1998, Furukawa *et al.*, 2003, Pintard *et al.*, 2003, Xu *et al.*, 2003). MEL-26 functions as a substrate-specific adaptor by recruiting MEI-1 into the complex for ubiquitin-mediated degradation (Furukawa *et al*, 2003, Pintard *et al.*, 2003, Xu *et al.*, 2003). Loss of *mel-26* activity results in mitotic defects due to ectopic MEI-1 (Clark-Maguire and Mains, 1994b).

Besides being regulated by the MEL-26/CUL-3 ubiquitination pathway, MEI-1 is also inactivated by other means. Phosphorylation of MEI-1 by the DYRK protein kinase MBK-2 is essential for MEI-1 degradation (Ming Pang *et al.*, 2004, Quintin *et al.,* 2003, Pellettieri *et al.,* 2003). Either inactivation of this kinase or disruption of the *mbk-2* phosphorylation site on MEI-1 prevents MEI-1 from being eliminated before mitosis (Stitzel *et al*., 2006). Furthermore, the protein level of phosphorylated MEI-1 reaches a peak just prior to the initiation of degradation, suggesting that MEI-1 phosphorylation may be a prerequisite for degradation (Stitzel *et al*., 2006). These findings reveal the significant effect of MEI-1 phosphorylation on its degradation.

The embryonic lethality of *mel-26(null)* is not complete at 15°C, suggesting the existence of a parallel pathway for MEI-1 degradation. Components of the anaphase promoting complex (APC) are also shown to be involved in MEI-1 inactivation/degradation. One APC subunit, MAT-2 (metaphase-anaphase transition) bound MEI-2 in a genome-wide yeast two-hybrid screen (Li *et al.*, 2004). Furthermore, embryonic lethality of *mel-26(null)* is significantly enhanced by mutants of *mat-2* or another APC subunit *emb-27* (abnormal embryogenesis) at 15°C, suggesting that APC and MEL-26 act redundantly to degrade MEI-1 (Lu and Mains, 2007). In addition, MBK-2 also seems to act redundantly with MEL-26 since *mbk-2* also enhances *mel-26(null).*

Taken together, inactivation of MEI-1/MEI-2 during the meiosis-to-mitosis transition is executed via multiple pathways including ubiquitin-mediated protein degradation, protein phosphorylation as well as regulation by certain cell cycle control components (Figure 3). To better characterize the mechanism of *mei-1* regulation, we aimed to identify new MEI-1 regulators by an RNAi screen.

1.4 RNAi screens for suppressors of *mei-1(gf)*.

RNA interference (RNAi) was a phenomenon first discovered in *C. elegans* (Fire *et al*., 1998). Although the underlying mechanism is not yet fully understood, it has been broadly applied to *lf* studies. By introducing double-strand RNA (dsRNA) into *C. elegans*, the expression of genes containing the sequence homologous to the dsRNA can be significantly and specifically reduced. Methods for delivering double-stranded RNA (dsRNA) into worms include: (1) injection of dsRNA into worms (Fire *et al*., 1998); (2) feeding animals bacteria producing dsRNA (Timmons *et al*., 2001); (3) soaking worms in dsRNA (Tabara *et al*., 1998); and (4) *in vivo* production of dsRNA from transgenic promoters (Tavernarakis *et al*., 2000). Since the C. *elegans* genome has been completely sequenced, RNAi can be used as a powerful tool in reverse genetics studies. Furthermore, the Ahringer lab constructed an RNAi feeding library that covers 87% of the predicted genes in *C. elegans* (Kamath *et al*., 2003). This library enabled us to screen a large portion of the genome to find MEI-1 interacting genes in a short period of time.

C. Birmingham in our lab performed an RNAi screen for candidate genes that function in *mei-1* regulation. After a screen of chromosome I genes in the library (2445 clones), one gene, *F16A11.3*, was identified as a suppressor of *mei-1(gf)* (Table 1). She also identified a known *mei-1(gf)* suppressor, *mei-2*, validating the screen.

F16A11.3(RNAi) thus acts as if it inhibits MEI-1 activity, although it has no effect on wild-type worms. However, feeding RNAi did not decrease the normal *meiotic* activity of MEI-1/MEI-2 since RNAi did not enhance a hypomorphic meiosis-defective allele of *mei-2*. This indicates that inhibition of MEI-1 activity functions only in mitosis but not in meiosis.

F16A11.3 encodes the R1 *regulatory* subunit of worm protein phosphatase 4 (PP4). In the *C. elegans* genome, two genes, *Y75B8A.30* and *Y49E10.3*, were identified as the *catalytic* PP4c subunit homologs and are designated as *pph-4.1* and *pph-4.2*, respectively (Sumiyoshi *et al.*, 2002). Three genes, including *F16A11.3* (*ppfr-1*, protein phosphatase four regulatory subunit), *D2092.2* (*ppfr-2*) and *Y71H2B.3* (*ppfr-3*), are designated as *regulatory* subunits (Table 2). Biochemical studies have shown that the PP4 *catalytic* subunits in mammals, flies and worms are localized at the spindle poles, the same region as ectopic MEI-1 (Brewis *et al*., 1993; Helps *et al.*, 1998, Sumiyoshi *et al.*, 2002). This supports the possibility that PP4 plays a role in MEI-1 regulation.

1.5 Protein phosphatase 4.

Protein phosphorylation-dephosphorylation is one of the most important cellular mechanisms for regulating protein activity, cell cycle and cell proliferation. Protein phosphorylation is catalyzed by kinases, which transfer phosphate groups from a high-energy compound, such as ATP, to specific amino acid residues (e.g., tyrosine, serine or threonine) on target proteins. Enzymes with the opposite activity, that is to remove phosphate groups from targets, are called protein phosphatases. The reversible phosphorylation-dephosphorylation processes provide an efficient way for proteins to reversibly change properties and exert diverse cellular functions.

PP4 belongs to the PPP family of serine/threonine phosphatases, and the amino acid sequences are highly conserved among different organisms (Cohen *et al.*, 2005). In all organisms investigated so far, including *C. elegans*, *Drosophila* and mammals, PP4 catalytic subunits localize to the centrosomes (Brewis *et al*., 1993; Helps *et al.*, 1998, Sumiyoshi *et al.*, 2002). Consistent with its localization, the function of PP4 involves regulating spindle formation and/or MT stability. A Drosophila mutant (*cmm*) with only 25% of normal PP4 protein level lacks MTs connecting chromosomes to the spindle poles, thus mitosis is disrupted (Helps *et al.*, 1998). One catalytic subunit of worm PP4, *pph-4.1*, is essential in centrosome maturation in mitosis while the other, *pph-4.2*, is dispensable (Sumiyoshi *et al.*, 2002). While the *C. elegans* work was done using RNAi, a deletion allele of *pph-4.1* is now available.

The high similarity between PP4c and PP2Ac (65% identical) indicates that they may share similar regulatory mechanisms. Since one possible mechanism to control the enzymatic activity of PP2Ac is by the association with its regulatory subunit, $PP2A_A$, it is quite likely that PP4c also forms a complex with regulatory subunits. Indeed, two regulatory subunits, PP4R1 (105 kDa) and PP4R2 (55 kDa) form distinct complexes with PP4c in mammals (Wada *et al*., 2001, Kloeker *et al.*, 1999, Hastie *et al*., 2000). Like the catalytic subunit PP4c, PP4R1 is also conserved among different species (e value -55, *C. elegans* compared to human). Sequence analysis has shown that, similar to $PP2A_A$, PP4R1 also has "heat repeat" regions, which may be important to PP4R1 protein conformation and association with other proteins. Like R1, the R2 subunit also associates specifically with PP4c and R2 colocalizes with PP4c to centrosomes of cultured human cells (Hastie *et al.*, 2000). Functions of R1 and R2 may involve inhibiting activity of the

catalytic subunit PP4c or narrowing substrate diversity *in vitro*, since purified PP4 complexes show little phosphatase activity towards substrates that are readily dephosphorylated by PP2A (Hastie *et al.*, 2000, Kloeker and Wadzinski, 1999). A third regulatory subunit, α-4, was originally identified as a component of the B-cell receptor complex that associates with the Ig α subunit (Inui *et al*., 1995, Kuwahara *et al.*, 1994). In contrast to the R1 and R2 subunits, which associate specifically with PP4c, α-4 binds to catalytic subunits of all three type 2A phosphatases (PP4, PP2A and PP6) in yeast-two-hybrid and in over-expression assays in mammalian cells (Chen *et al*., 1998, Nanahoshi *et al.*, 1999).

In my work, I demonstrated that mutants and/or RNAi of three PP4 subunits, including one catalytic subunit, *pph-4.1,* and two regulatory subunits, *ppfr-1* and *ppfr-3,* (which correspond to the R1 and α-4 regulatory subunits of mammalian PP4, respectively), suppress embryonic lethality caused by ectopic mitotic MEI-1. RNAi to the other PP4 subunits (PPH-4.2 and R2/*ppfr-2*) do not suppress ectopic MEI-1. I also tried to determine the underlying mechanism of how loss of the *PP4* genes suppresses *mei-1(gf)*. It is unlikely that reduction in PP4 activity increases general MT stability, making MTs resistant to ectopic MEI-1 severing. Another model, which proposes loss of PP4 phosphatase results in higher levels of MEI-1 phosphorylation, leading to increased degradation, also does not seem to be the case. Instead, reciprocal co-immunoprecipitation experiments indicate that PP4 may regulate MEI-1 activity via direct binding.

Figure 1: The meiotic and mitotic spindles are different as shown by anti-α-tubulin staining.

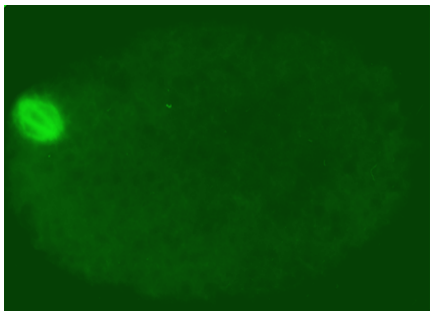

Meiosis:
Metaphase I

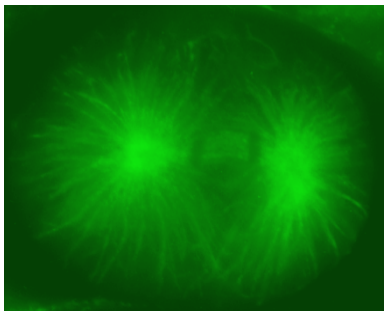

Mitosis: Metaphase
of the First Cleavage

Figure 2: Spindle morphology and MEI-1 localization during the first mitotic cleavage in wild type and *mei-1(gf)*.

MTs are revealed by anti-α-tubulin staining while MEI-1 is detected with anti-MEI-1. Note the lack of MEI-1 staining in wild-type mitosis and the small and misplaced spindles characteristic of *mei-1(gf)* and *mel-26*.

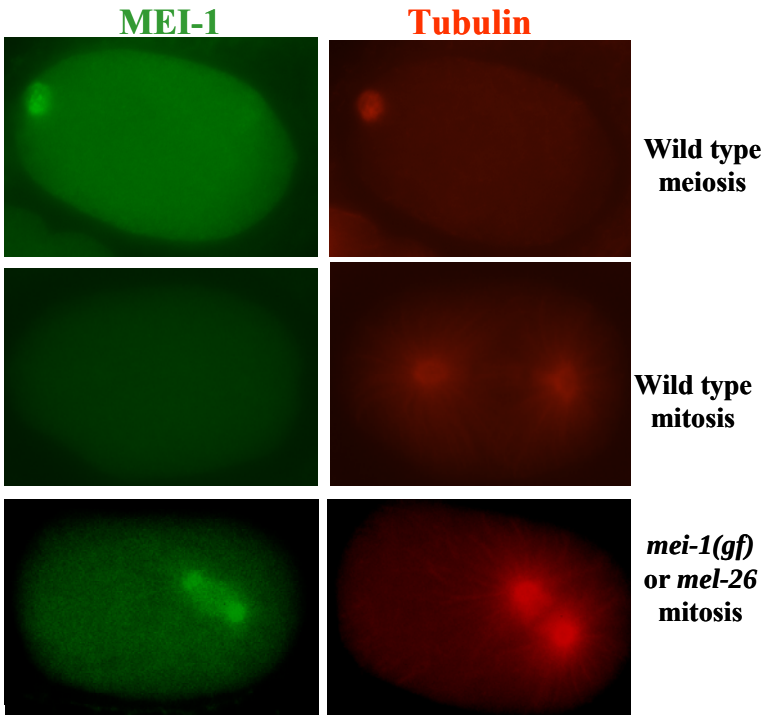

Figure 3: post-meiotic MEI-1 degradation pathways

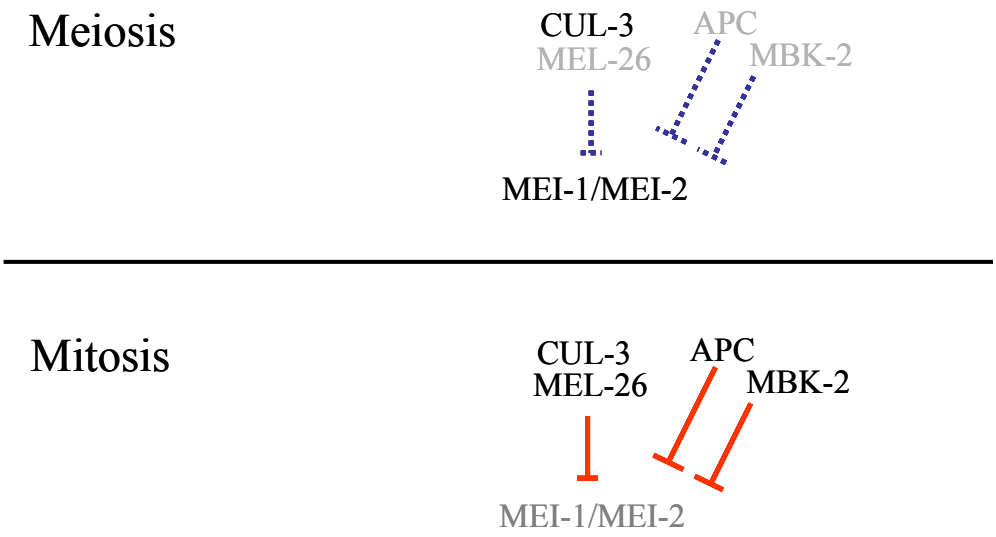

Dash or gray lettering indicates absence of the protein or no activity. Solid indicates presence of the protein or high activity. "----I " represents negative interaction.

At meiosis, all MEI-1/ MEI-2 degradation pathways are inactive, resulting in high levels of MEI-1/ MEI-2. At mitosis, MEI-1/ MEI-2 are degraded by redundant pathways, mediated by CUL-3/ MEL-26, MBK-2 and APC.

Table 1: *F16A11.3(ppfr-1)* suppresses post-meiotic *mei-1* at 20°C.

F16A11.3 was initially identified by C. Birmingham.

Genotype	% Hatching
Wild type	99
Wild type; *F16A11.3* (feed)	98
mei-1(gf)	5
mei-1(gf); *F16A11.3* (feed)	20
mel-26(lf)	1
mel-26(lf); *F16A11.3* (feed)	14
mei-2(lf)	54
mei-2(lf); F16A11.3 (feed)	53

Table 2: Components of *C.elegans* PP4

		Encoding genes
Catalytic subunits	Catalytic subunit 1	*Y30A8.5 (pph-4.1)*
	Catalytic subunit 2	*Y49E10.5 (pph-4.2)*
Regulatory subunits	Regulatory subunit 1	*F16A11.3 (ppfr-1)*
	Regulatory subunit 2	*D2092.2 (ppfr-2)*
	Regulatory subunit 3	*Y71H2B.3 (ppfr-3)*

Chapter Two: Materials and Methods

2.1 Nematode culture and strains.

C. elegans were cultured under standard conditions (Brenner, 1974) unless otherwise specified. Strains used in my studies included wild type N2 (var. Bristol), *mei-1(ct46gf) unc-29(e1072)*, *mel-26(ct61gf* and *ct61sb4) unc-29(e1072)*, *tba-2(sb51gf)*, *ppfr-1(tm2180)*, *zyg-9(b244)*, *pph-4.1(tj19* and *tj20)*, and *unc-116(rh24)*. Lethal strains were balanced with the translocation *hT2[myo-2:: GFP] (I;III)* or *hT2[bli-4(e937) let(h661)] (I;III)*. Temperature-sensitive strains were raised at 15°C until the L4 stage and up-shifted to 20°C or 25°C for 24 hours before embryos were collected. Hatching rates were scored based on complete broods of more than 500 embryos from at least 4 hermaphrodites. Procedures to make *mei-1(gf) ppfr-1(tm2180)* double mutant are included in Figure 5. Primers used to confirm *tm2180* deletion are as follows:

ppfr-1-D-F: CAAGTTCGACAATCTTATGTTTC

ppfr-1-D-R: AACTCGCATTACTGCGGAATTT

2.2 RNAi.

RNA-mediated interference was performed using both the feeding (Timmons *et al*., 2001) and injection (Fire *et al*., 1998) methods. The targeted sequences were searched using BLAST against the *C. elegans* genome to ensure the specificity of RNAi effect. For injection, RNA was *in vitro* transcribed using the Megascript system (Ambion, Austin,TX) and purified and annealed according to previous descriptions (Fire *et al*., 1998). dsRNA was microinjected at a concentration of ~2 mg/ml into the gonads or the intestines of young adult hermaphrodites, and the F1 progeny were collected 20-44 hours after injection to determine hatching rates. For RNAi feeding, L4 larvae were placed on

plates seeded with dsRNA producing bacteria (Timmons *et al*., 2001) and transferred to fresh plates every 24 hours until egg-laying ceased. The first broods were not included for scoring hatching rates.

2.3 Cloning *pph-4.1, pph-4.2* and *ppfr-3.*

The fragments of *pph-4.1, pph-4.2* and *ppfr-3* were amplified from embryonic cDNA generated by RT-PCR (Invitrogen Superscript III) and cloned into the L4440 vector individually. Constructs were confirmed by sequencing and transformed into both JM109 and HT115 (DE3) bacteria.

List of primers:

pph-4.1 forward: TGGCTCTGGCGTGCACCGAC

pph-4.1 reverse: TCGATAACCTGGACGTTGC

pph-4.2 forward: GATCAATTAGGCCCGAACG

pph-4.2 reverse: CACAGATTGTGACCGGTGT

ppfr-3 forward: TGAAGACGTTCCAACAAACTCGCTG

ppfr-3 reverse: CTCCTCGTAACATCTTTCACTCCAG

2.4 Indirect immunofluorescence microscopy

Embryos were processed by the freeze-cracking method (Miller 1995) and fixed with methanol-acetone (Kemphues *et al*., 1986). MEI-1 and α-tubulin localization was determined as described (Srayko *et al*., 2000; Lu and Mains, 2005). Photographs were taken by a Hamamatsu ORCA-ER digital camera equipped on a Zeiss Axioplan II microscope. The same settings were used for all anti-MEI-1 immunofluorescence. To define if an embryo is positive or negative for ectopic MEI-1, MEI-1 localization at the spindle poles vs. in the cytoplasm was analyzed. When more MEI-1 localize at the

spindle poles than in the surrounding cytoplasm, this embryo is scored as positive (Figure 6B).

2.5 Scoring spindle morphology.

L4 larvae were raised at 15°C and shifted to the experimental temperatures 24 hours before dissection. One-cell embryos were dissected and mounted as in previous descriptions (Sulston *et al*., 1983). The first mitotic division was recorded by time-lapse Nomarski microscopy (Gomes *et al*, 2001) by using a Zeiss Axioplan 2 microscope. The microscope room was adjusted to the experimental temperatures during the observation period. To score the fractional spindle length and orientation, measurements were made at nuclear envelope breakdown (NEBD) and cytokinesis, which is indicated by the appearance of the cleavage furrow. The fractional spindle length was defined as the ratio of distance between two spindle poles to the length of the A-P axis. The spindle orientation was defined as the angle made by the line connecting two spindle poles and the A-P axis (Figure 4).

2.6 Co-immunoprecipitation.

Purified rabbit anti-MEI-1, anti-PPH4.1 as well as purified rabbit IgG (ZYMED, negative control) were cross-linked to protein-A-agarose beads with dimethylpimelimidate (DMP), using a protocol improved from description of Wijk *et al*. (2004). Generally, the antibody was incubated with protein-A-agarose beads for 1 hour at room temperature and cross-linked with 20mM DMP (freshly made) in 0.1 M $Na_2B_4O_7$ (pH 9.0) for 30 min at room temperature. To quench excess DMP, the beads were allowed to settle and incubated with 0.1M $Na_2B_4O_7$ without DMP for 30min, followed by two rounds incubation with 0.2M Tris-HCl (pH8.0), 1 hour for each round. The beads

were quickly washed once with 0.1M glycine (pH 2.3), twice with 0.1M Tris-HCl (pH 8.0), and resuspended in Phosphate Buffered Saline (PBS) buffer to make 1:1 slurry. Crosslinked antibodies were stored for later use at 4°C in PBS containing 0.02% NaN_3.

Liquid culturing of *C. elegans* was performed as in previous descriptions (Lewis *et al.*, 1995). Cytosolic extracts were prepared according to a method from the Schedl Lab (http://www.genetics.wustl.edu/tslab/protocols.html). Generally, 1 to 3 ml of packed worms were washed twice with PBS, twice with ddH_2O, and finally resuspended in 5 ml HB buffer (homogenization buffer, recipe: 15 mM Hepes pH 7.6, 10 mM KCl, 1.5 mM $MgCl_2$, 0.1 mM EDTA, 0.5 mM EGTA, 44 mM Sucrose; add fresh: 1 mM DTT and protease inhibitors (Complete, Mini, EDTA-free, Roche)). Lysates were prepared by sonication and cleared by spinning at 10000 g for 10 min at 4°C. For each IP, 0.5 ml lysate was incubated with 50 µl antibody coupled agarose either at room temperature for 2 hours or at 4°C overnight. After being washed six times with IP buffer (HB buffer with 100 mM NaCl), proteins were eluted in 0.1 M glycine (pH 2.3) followed by 2X-SDS (sodium dodecyl sulphate) sample buffer and were separated by SDS-PAGE for western blot analysis. For mass-spec analysis, proteins pulled down by anti-MEI-1 were separated by SDS-PAGE (12%). The proteins with molecular weights falling in the range of 33kDa to 45kDa were collected and the in-gel samples were sent to the Southern Alberta Mass Spectrometry Centre (http://www.sams.ucalgary.ca/v3/) for identification by Matrix-assisted laser desorption/ionization (MALDI).

Figure 4: Scoring the fractional spindle length and orientation.

mei-1(gf) at 20°C, DIC time-lapse

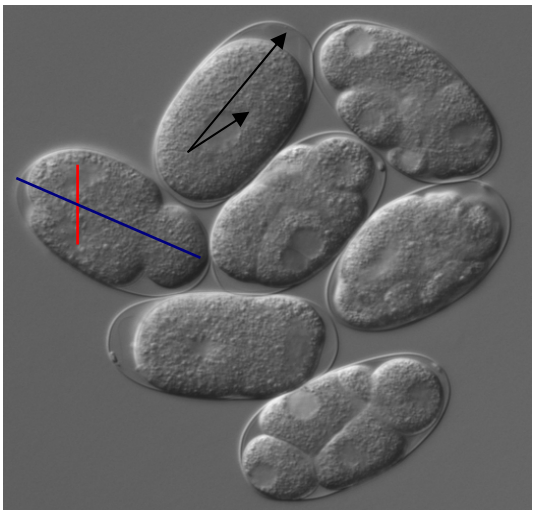

fractional spindle length = distance between spindle poles (red line) divided by the length of the A-P axis (blue line)

spindle orientation = angle between A-P axis and a line connecting two spindle poles (black lines)

Figure 5: Construction of the *mei-1(gf) ppfr-1(tm2180)* double mutant.

The two genes are tightly linked, separated by 1.05cM. The original *tm2180* strain included an unrelated sterile (Ste) mutation that was crossed off as indicated in the second generation.

A Crossing off the sterile mutation linked to *ppfr-1(tm2180)*

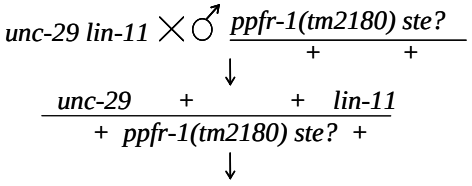

Pick Lin, non-Unc progeny
Confirm *tm2180* by PCR
Keep those do not segregate Ste progeny

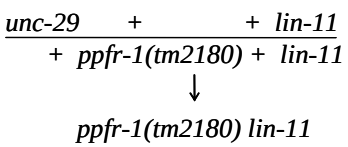

B Construction of the *mei-1(gf) ppfr-1(tm2180)* double mutant.

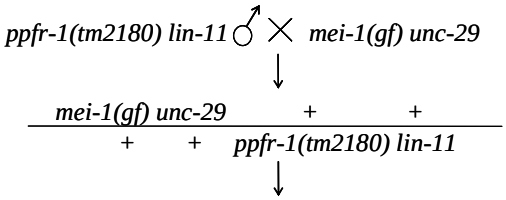

Pick Unc progeny , keep those segregate Lin progeny, confirm *tm2180* by PCR

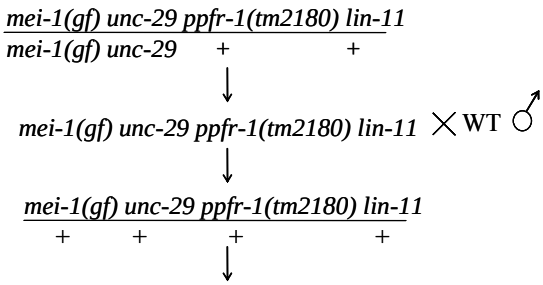

Pick Unc non-Lin progeny, keep those are homozygous for *tm2180* by PCR

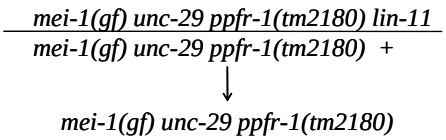

Chapter Three: Results

3.1 Loss of three PP4 subunits (*ppfr-1*, *ppfr-3*, and *pph-4.1*) suppresses *mei-1(gf)* during mitosis.

The *ppfr-1* regulatory subunit was identified as a *mei-1(gf)* suppressor by C. Birmingham in a chromosome I RNAi screen. At 20°C, hatching was increased from 5% to 20% (Table 1). Since in mammals the highly-conserved PP4 complex is composed of both catalytic and regulatory subunits, it is likely that in worms, *ppfr-1* also acts in concert with one or both of the two *C. elegans* PP4 catalytic subunits. I knocked down each of the PP4 catalytic subunits (*pph-4.1* and *pph-4.2)* in the *mei-1(gf)* genetic background by RNAi and scored for suppression of lethality caused by ectopic MEI-1. Since *pph-4.1* and *pph-4.2* are similar to each other (74% base pair identity, with a maximum length of 15 identical nucleotides), the 5' end sequences, with no significant similarity were chosen to construct the plasmids for gene-specific RNAi and thus the possibility that RNAi to *pph-4.1* was also targeting *pph-4.2* and *vice versa* was avoided. My RNAi results showed that knocking down only one of these two catalytic subunits, *pph-4.1,* rescued embryonic lethality, and this was to a similar level as *ppfr-1(RNAi)* (Table 3A). Simultaneous RNAi against both *pph-4.1* and *ppfr-1* showed the same rescuing capacity as either alone, suggesting that the PPFR-1 regulatory subunit acts only in concert with the PPH-4.1 catalytic subunit to rescue lethality. In contrast, RNAi to the second catalytic subunit, *pph-4.2*, did not rescue *mei-1(gf)* lethality nor did it alter *ppfr-1(RNAi)* rescue of *mei-1(gf).* Similarly, *mel-26* was also rescued by knocking down *pph-*

4.1 but not *pph-4.2*, suggesting that the above findings were not specific to *mei-1(gf)* (Table 3A).

I also examined RNAi to the two other predicted regulatory subunits of PP4, *ppfr-2*/PP4R2 and *ppfr-3*/PP4α-4. RNAi against *ppfr-3*, which interacted with *pph-4.1* in the global *C. elegans* yeast two-hybrid screen (Li *et al.*, 2004), resulted in embryonic lethality in the wild-type background (Table 3B). We did not investigate the cause of this lethality. When corrected for this background lethality, *ppfr-3(RNAi)* also suppressed *mei-1(gf)* (Table 3A). Thus it seems that *pph-4.1* works in concert with *ppfr-1* and *ppfr-3* to regulate *mei-1*. In contrast, RNAi to the remaining PP4 regulatory subunit, *ppfr-2,* did not suppress *mei-1(gf)*, either alone or in concert with *ppfr-1* (Table 3A).

The RNAi results were promising and further confirmed by using mutants, which were inherently less variable compared to RNAi. Recently a deletion of *ppfr-1* became available through the National Bioresource Project for the Nematode (Japan) (Gengyo-Ando and Mitani 2000). *tm2180* is a 1027 bp deletion mutation of *ppfr-1* that removes three exons at the 3' end of the gene. The mutation was outcrossed 5 times and then a crossover between the flanking markers *unc-29* and *lin-11* was used to remove a closely linked sterile mutation (Figure 5). The strain carrying the "clean" *tm2180* allele appeared to be nearly wild type, with 85% hatching (Table 4, the embryonic lethal phenotype was not examined). *ppfr-1* is closely (1.05 cM) linked to *mei-1*, and I crossed *tm2180* on to a *mei-1(gf)* bearing chromosome (Figure 5) and scored the hatching rate. As shown in Table 4, hatching rates were similar to those from *ppfr-1(RNAi)*. This finding not only validated my RNAi experiments but also suggested the *lf* nature of the *ppfr-1* deletion

mutation. Notably, complete loss of *ppfr-1* does not suppress *mei-1(gf)* at 25°C, indicating that *ppfr-1* is not a bypass suppressor.

We also obtained deletion alleles of *pph-4.1*, and the results will be discussed later.

3.2 Exploring the mechanism of PP4 suppression of *mei-1(gf)*.

In the previous section, I found lethality of ectopic mitotic MEI-1 caused by *mei-1(gf)* or *mel-26* can be suppressed by *pph-4.1*, *ppfr-1* or *ppfr-3* RNAi. In the next section, I will explore the underlying mechanism of this rescue, that is, whether ectopic MEI-1 is degraded, inactivated or mislocalized when PP4 levels are reduced.

3.2.1 Model One: PP4 (+) reduces general MT stability.

Based on previous publications, PP4 is involved in regulating spindle formation and/or MT stability in both *Drosophila* (Helps *et al.*, 1998) and *C. elegans* (Sumiyoshi *et al.,* 2002). It was also shown that in *C .elegans*, MEI-1/MEI-2 have katanin-like MT-severing activity (Srayko *et al*.,2000, Srayko *et al*., 2006, McNally *et al*., 2006). Based on these findings, the first model I proposed was that PP4 regulates MT stability, rather than regulating MEI-1 directly, such that loss of PP4 results in MTs that are generally more stable, and thus are resistant to ectopic MEI-1 severing. A quick and easy way of testing this model was to determine if there were genetic interactions between PP4 and mutations in other genes that destabilize MTs by mechanisms other than severing. *sb51* is a *gf* allele of *tba-2* (one of the two embryonically expressed α-tubulin isotypes) with a poisonous activity that reduces MT stability (Lu and Mains 2005, Phillips *et al.*, 2004). If depletion of PP4 makes MT stronger, thus refractory to MEI-1/MEI-2 severing, it should also rescue the *tba-2(sb51)* mutant, which has compromised MT stability. However, this was

not the case as *ppfr-1(RNAi)* did not rescue *tba-2(sb51)* lethality (Table 5A). Similar results were obtained when I tested other mutants with reduced MT stability, including the kinesin heavy chain mutant *unc-116* (Patel *et al*., 1993, Yang *et al*., 2005) and *zyg-9* (Matthews *et al.*, 1998), which encodes a MT-stabilizing MAP (Table 5A).

γ-tubulin and MEI-1 both are involved in increasing the number of MT ends during normal meiosis, which can nucleate new MTs (Srayko *et al*., 2006, McNally *et al*., 2006). If this also occurs during mitosis in *mei-1(gf)*, it is possible that loss of PP4 suppresses the effect of too much MEI-1 by reducing microtubule nucleation from the parallel γ-tubulin pathway. If so, then *tbg-1(RNAi)* should also rescue *mei-1(gf)*. Again, results didn't support this hypothesis (Table 5B).

Taken together, my results with *tbg-1* and the MT-destabilizing mutants suggest that suppression of *mei-1(gf)* by PP4 regulated MT stability/nucleation is unlikely.

3.2.2 Model Two: PP4 (+) inhibits degradation of post-meiotic MEI-1.

Since in wild-type embryos, the cytoplasmic MEI-1 level drops dramatically when meiosis is completed, I asked if PP4 normally inhibits MEI-1 degradation (Figure 6A). This model is based on the observation that phosphorylation is a prerequisite to ubiquitin-mediated degradation (Winston *et al*., 1999); thus loss of PP4 would increase levels of the phosphorylated form of MEI-1, favouring MEI-1 degradation. If this model is correct, inhibition of PP4 in *mei-1(gf)* should result in an increase in the number of MEI-1 negative embryos, which is closely correlated with the hatching rate (Lu and Mains, 2007).

To address this possibility, I performed immunochemical staining of *mei-1(gf)* and *mei-1(gf); ppfr-1(RNAi)* embryos using purified anti-MEI-1 antibody and compared

the percentage of early mitotic embryos with and without ectopic MEI-1. My results argued against the degradation model. Of the 88 one- and two-cell stage embryos from the *mei-1(gf); ppfr-1(RNAi)* mothers at 20°C, none were scored negative for post-meiotic MEI-1 (Figure 6B). This was dissimilar to the expectation of our model (13% hatching, so ~12 embryos should have been negative for ectopic MEI-1) and almost the same as the *mei-1(gf)* controls (3% negative for ectopic MEI-1). Similarly, the localization (spindle pole vs. cytoplasm) and the MEI-1 levels seen on Western blots were also not altered (data not shown).

Since phosphorylation of MEI-1 by the MBK-2 is essential for its degradation (Ming Pang *et al.*, 2004, Quintin 2003, Pellettieri 2003), I also did immunochemical staining with anti-Phospho-MEI-1 (Stitzel *et al.*, 2006). As shown in Table 6B, phosphorylation of post-meiotic MEI-1 by MBK-2 is indistinguishable in *mei-1(gf)* and *mei-1(gf) ppfr-1(tm2180)* embryos at 25°C (For a more detailed discussion of this result, see Chapter 4).

To summarize, PP4 does not appear to regulate MEI-1 at the level of protein degradation or localization, although subtle changes cannot be ruled out.

3.2.3 Model Three: PP4 regulates MEI-1 activity directly and thus the spindle morphology.

Although the MEI-1 protein level and localization pattern were not changed by removing PP4, the morphology of mitotic spindles indeed looked different in embryos with ectopic MEI-1 that were treated *ppfr-1(RNAi)* and then stained with anti-α-tubulin (Figure 7). At 20°C, the one-cell *mel-26* embryos can be divided into the following

groups based on spindle morphology: embryos with small spindles inclined away from the A-P axis (35%), embryos with small but properly orientated spindles (53%), and embryos with wild-type spindles (12%). When PP4 was inactivated by *ppfr-1(RNAi)*, the percentage of embryos with wild-type spindles increased from 12% to 49%. Similar results were obtained when *mei-1(gf)* was used instead of *mel-26* (data not shown).

This data might be misleading, as these fixed embryos only represented one time point of the first division and compression of embryos during fixation might alter spindle orientation. A more detailed characterization of the spindle morphology was carried out by recording the first division of living embryos with Normaski microscopy. The fractional spindle length and orientation at two time points, nuclear envelope break down (NEBD) and cytokinesis, were measured as previously described (Gomes *et al.*, 2001). For scoring spindle orientation, embryos were divided into four groups based on the angles formed by the spindle and A-P axis, including those that had a normal orientation (< 10° from the A-P axis), slightly inclined (11° to 30°), moderately inclined (31° to 60º), and steeply inclined (61° to 90°). At 20°C, all wild-type embryos had the mitotic spindles positioned properly at the onset of cytokinesis (*i.e.,* < 10°). In *mel-26*, 80% of the embryos had properly orientated spindle, 14% slightly inclined, 6% moderately inclined and no steeply inclined at cytokinesis (Figure 8). Although RNAi to *pph-4.1* rescued lethality of *mel-26*, loss of *pph-4.1* also frequently resulted in failure in mitosis and formation of tetra-polar spindles (Sumiyoshi *et al*., 2002), making it difficult to analyze spindle morphology. Thus I decreased *ppfr-1* instead of *pph-4.1* to knock down the PP4 phosphatase. No dramatic difference was found between *mel-26; ppfr-1(RNAi)* and *mel-26* embryos in spindle orientation at NEBD or cytokinesis (Figure 8).

As another metric of the spindle function, I measured the maximum length of the first cleavage spindle. The wild-type spindles had an average length of 58 $\pm$ 2 percent of egg length (Figure 9). That of *mel-26* was shorter, 48 $\pm$ 5 percent of egg length, but the same value was obtained for *mel-26* suppressed by *ppfr-1(RNAi)* (p-value: 0.618).

The above results indicate that any differences between *mel-26; ppfr-1(RNAi)* and *mel-26* were likely so subtle as to be undetectable. However, the difference between wild type and *mel-26* was also not prominent, for example even though only 1% of *mel-26* embryos hatched, 80% of the *mel-26* embryos had normal spindle orientation (*i.e.,* < 10°) at the onset of cytokinesis (Figure 8). Therefore, I chose a more sensitized condition that might better distinguish the differences, if there were any, between wild type and *mel-26*. I cultured worms at the more restrictive temperature (25°C). This condition did not affect spindle orientation of wild type but dramatically exacerbated defects of *mel-26*, of which only 4% had normal spindle orientation at cytokinesis while 66% had steeply inclined spindles (Figure 10). As I expected, PP4 RNAi corrected spindle orientation to some extent relative to *mel-26*. In *mel-26; ppfr-1(RNAi)* embryos at cytokinesis, there was an increase from 3% to 13% in the proportion of properly orientated spindles and an increase from 0% to 12% in slightly inclined ones when scored (p-value: 3×10^{-2}) (Figure 10). The fractional spindle length of *mel-26* at cytokinesis did increase from 34 $\pm$ 3 percent of egg length to 38 $\pm$ 5 (p-value: 3×10^{-4}) (Figure 11). Although this is still different from normal (56 $\pm$ 3), it is very obvious that the spindle morphology became better by reducing PP4 activity.

Taken together, these findings supported the idea that reduction in PP4 suppressed MEI-1 toxicity and increased the percentage of embryos with wild-type spindles at the

end of the first division. Although no significant changes were observed in spindle morphology at 20°C, this could be explained by the model that at the end of the first division, embryos were extremely sensitive to MEI-1 activity/spindle morphology. A slight change in spindle length/orientation, which might be barely detected by our methods of scoring, could decide the fate of embryos. This idea was also supported by the fact that at 20°C, difference in hatching rates of *mel-26* and wild type differed by 100 fold, but the difference in spindle morphology was not as dramatic. This led me to propose a third model, which proved to be more consistent with my data: PP4 (+) might counteract an unknown kinase required to inhibit MEI-1. Loss of PP4 would shift MEI-1 to the catalytically inactive phosphorylated form, restoring normal mitotic spindle morphology (Figure 12). Next I would like to address if PP4 regulated MEI-1 directly.

3.2.4 PP4 may regulate MEI-1 directly.

If PP4 regulates MEI-1 via certain intermediates, reducing the intermediates that act in the same sense as PP4 (*i.e.*, their wild-type products function to inhibit MEI-1 activity) should rescue *mei-1(gf)* to a similar level as PP4 RNAi. The products of eight genes are reported to show physical interaction with *pph-4.1* in a large yeast two-hybrid interaction screen that included the majority of *C. elegans* genes (Li *et al.*, 2004). Six are included in the RNAi feeding library (Kamath *et al*., 2003). *plk-1*(polo-like kinase 1) was also tested as a candidate, as centrosomal localization of *plk-1* was altered by knocking down PP4 (Sumiyoshi *et al*., 2002). As shown in Table 7, RNAi to none of these genes rescued *mei-1(gf)*.

As mentioned previously, the worm PPH-4.1 catalytic subunit localizes to the spindle poles (Sumiyoshi *et al.*, 2002), one of the locations where ectopic MEI-1 is found

in *mei-1(gf)*. This suggests their interaction might be via direct binding. To address this possibility, I did reciprocal co-immunoprecipitation (co-IP) experiments with purified rabbit antibodies against PPH-4.1 (kindly provided by Dr. A. Sugimoto, Laboratory for Developmental Genomics, RIKEN Center for Developmental Biology, Japan) and MEI-1. As expected, PPH-4.1 and MEI-1 were apparently pulled down by each other (Figure 13A), but not by a rabbit IgG control antibody (Figure 13B). However, the results were not consistent. Overall, in 3 out of 7 experiments, a band at the molecular weight corresponding to PPH-4.1 was pulled down by anti-MEI-1, while 2 out of 3 times a band at the molecular weight where MEI-1 was expected was pulled down by anti-PPH-4.1 (Table 8). I also tried to use mass spectrometric strategy to confirm the existence of PPH-4.1 in the protein complex from anti-MEI-1 IP (This round of IP was not included in Table 8, as all of the protein was used for Mass Spec instead of western blot). Unfortunately the result was negative (Table 9). The failure of this experiment might be caused by low abundance of PPH-4.1 in the PPH-4.1-MEI-1 complex, as shown by western blot (Figure 13A). It was also possible that PPH-4.1 was not successfully co-purified with MEI-1 for this specific experiment, since I got inconsistent results when I did co-IP with anti-MEI-1.

Although it seemed to be easier to perform IP with anti-PPH-4.1 rather than MEI-1, the limited amount of anti-PPH-4.1 (contributed by Dr. Sugimoto) limited my ability to optimize the experiments with anti-PPH-4.1. To test if the inconsistent results were due to low abundance of either protein, I increased the input protein by 10 fold and found no improvement (Table 8). I tried various other conditions to optimize the experiment, including changing the primary antibody incubation times and using *mei-1(gf)* as the

worm input since this strain has more total MEI-1. The inconsistent results suggested the MEI-1/PPH-4 binding may be transient or unstable.

Table 3: RNAi against *pph-4.1*, *ppfr-1* and *ppfr-3* rescues *mei-1(gf)* lethality.

A. RNAi to *pph-4.1*, *ppfr-1* and *ppfr-3* increased hatching of *mei-1(gf)* and *mel-26*. Hatching rates, at 20°C, are reported.

RNAi to *mei-1(gf)*	% Hatching
mei-1(gf) No RNAi	1.0
pph-4.1 (inject)	19.2
pph-4.2 (inject)	3.0
pph-4.1+ pph-4.2 (inject)	11.0
ppfr-1 (inject)	15.5
ppfr-2 (inject)	1.3
ppfr-1+ppfr-2 (inject)	12.2
ppfr-3 (feed)	14.5[a]
pph-4.1+ ppfr-1 (inject)	21.6
pph-4.2+ ppfr-1 (inject)	13.1
RNAi to *mel-26*	% Hatching
mel-26 No RNAi	1.0
pph-4.1 (feed)	14.0
pph-4.2 (feed)	2.8
ppfr-1 (feed)	10.0
ppfr-2 (feed)	0.1
ppfr-3 (feed)	8.3[a]

[a] Corrected for the 20% lethality caused by *ppfr-3(RNAi)* shown below.

B. RNAi against *ppfr-3* caused embryonic lethality on its own.

	ppfr-3(RNAi) to wild type	% Hatching
wild type	0	100
	Feed	80
	Inject at 0.2 μg/μl	14
	Inject at 1.5 μg/μl	6

Table 4: Suppression of *mei-1(gf)* lethality by *ppfr-1(RNAi)* was confirmed by using the *ppfr-1(tm2180)* mutant.

Strain	% Hatching		
	Temperature °C		
	15	20	25
mei-1(gf)	13	1	0
mei-1(gf)/+	84	31	0.2
ppfr-1(tm2180)	90	86	81
mei-1(gf) ppfr-1(RNAi)	51	14	0
mei-1(gf) ppfr-1(tm2180)	57	7	0
mei-1(gf) ppfr-1(tm2180)/+ +	85	45	0.4
mei-1(gf) +/+ ppfr-1(tm2180)	90	69	0.4
mel-26(ct61)/+	86	50	0.6
mel-26(ct61) +/+ ppfr-1(tm2180)	88	72	1.3
mei-1(gf) ppfr-1(tm2180)/ mei-1(gf) +	30	12	ND[a]

[a] Not determined.

Table 5: PP4 may not regulate MT stability or nucleation.

A. *ppfr-1* does not interact with *unc-116, tba-2/+* or *zyg-9.*

Strain	Temperature °C	% Hatching No RNAi	% Hatching *ppfr-1(RNAi)* (feed)
mei-1(gf)	20	1.5	12
unc-116(rh24)	20	17	17
tba-2(sb51)/+	20	21	19
zyg-9(b244)	22.5	43	36

B. RNAi against *tbg-1*did not rescue *mei-1(gf)* lethality at 20°C.

% Hatching	control	*tbg-1(RNAi)*
wild type	100	23
mei-1(gf)	1.2	0.3

Table 6: PP4 does not counteract MBK-2

A. PP4 RNAi did not rescue *mbk-2(dd5)* or *emb-27* at 20°C. Embryos were collected 20 hours post injection

Strain	% Hatching					
	No RNAi	*pph-4.1*	*pph-4.2*	*ppfr-1*	*ppfr-2*	*pph-4.1+ ppfr-1*
mbk-2(dd5)	60	47	55	31	69	30
emb-27	59	43	58	52	49	50
mbk-2(dd5); emb-27	3	3	3	2	2	2

B. In *mei-1(gf)* embryos, phosphorylation of post-meiotic MEI-1 by MBK-2 is the same in the presence or absence of PP4.

25°C anti-P-MEI-1	P-MEI-1 + 1-cell	P-MEI-1 + 2-cell	P-MEI-1 +, Meiosis
mei-1(gf)	60/62	17/17	22/30
mei-1(gf) ppfr-1(tm2180)	37/39	16/16	6/21

Table 7: List of genes that show physical interactions with PPH-4.1.

A. RNAi to genes with yeast two-hybrid interactions.

Y2H bait *pph-4.1*	Target	Description	Hatching of RNAi worms compared to those without RNAi (20°C)		
			wild type	*mei-1(gf)*	*mel-26*
	Y53F4B.22	actin and related proteins	0.9	0.1	0.1
	Y54E10A.2	*cogc-1*(Conserved Oligomeric Golgi Component)	1.0	0.5	1.0
	C28H8.12	*dnc-2* (DyNactin Complex component)	ND[a]	ND	ND
	F10C1.2a	intermediate filament B	1.0	2.5	1.0
	F25B3.5	novel	1.0	1.5	1.5
	EEED8.3	novel	1.0	2.0	1.5
	W10G11.20	novel	ND[a]	ND	ND

In each strain, hatching of RNAi worms is compared to those of non-RNAi ones and the ratios are shown in the table.

[a] Not determined as the gene was not in the feeding library.

B. PP4 does not regulate MEI-1 via PLK-1.

plk-1(RNAi) feeding time	3.5 hrs	8 hrs	12 hrs	>48 hrs
wild type	100	34	25	0
mei-1(gf)	1.7	1.6	1.1	0

At 20°C, if *plk-1* and *mei-1(gf)* cause lethality independently of each other, the expected hatching of *plk-1*(RNAi, 8 hrs) to *mei-1(gf)* is 0.6% (0.34×0.017). However, 1.6% was observed instead of 0.6%. Thus it seems *plk-1*(RNAi) might have rescued *mei-1(gf)* (1.6/0.6, that is about 3 fold), but not as much as PP4 (RNAi) (>15 fold).

Table 8: Summary of co-IP results

	Blot positive for		Volume of protein A agarose (µl)	Genotype	Incubation
	PPH-4.1	MEI-1			
anti-MEI-1	+	+	50	wild type	4°C overnight
anti-MEI-1	+	+	50	wild type	4°C overnight
anti-MEI-1	+	+	50	*mei-1(gf)*	4°C overnight
anti-MEI-1	-	+	50	wild type	4°C overnight
anti-MEI-1	-	+	50	*mei-1(gf)*	4°C overnight
anti-MEI-1	-	+	50	wild type	4°C overnight
anti-MEI-1	-	+	500	wild type	Room Temp 2hrs
anti-PPH-4.1	+	+	50	wild type	4°C overnight
anti-PPH-4.1	+	+	50	*mei-1(gf)*	4°C overnight
anti-PPH-4.1	-	-	50	wild type	4°C overnight

Table 9: Mass Spectrometry of IP bands

Proteins pulled down by anti-MEI-1 were separated by SDS-PAGE. The proteins with molecular weights falling in the range of 33kDa to 45kDa were collected for identification by mass spectrometry. As shown in this table, PPH-4.1(37 kDa) was not identified by this experiment.

	Gene	Description
1	M03F4.2	*act-4*, an actin isoform that is most similar to *act-2* in amino acid sequence
2	T04C12.4	*act-3*, an invertebrate actin that is highly similar to ACT-1, ACT-2, and ACT-4 and functions in body wall muscle
3	T04C12.5	*act-2*, an invertebrate actin that may function specifically in the pharynx.
4	C26C6.7	novel
5	H04J21.3	*gip-1* (Gamma-tubulin Interacting Protein)
6	T01D3.2	novel
7	F08D12.10	*sdz-9* (SKN-1 Dependent Zygotic transcript)
8	F22F4.3	*klp-13* (Kinesin-Like Protein)
9	F49H6.5	novel
10	C16A11.6	novel

Figure 6: PP4 does not regulate MEI-1 degradation.

A. **Model Two: PP4 is involved in mel-26 pathway to degrade MEI-1**.

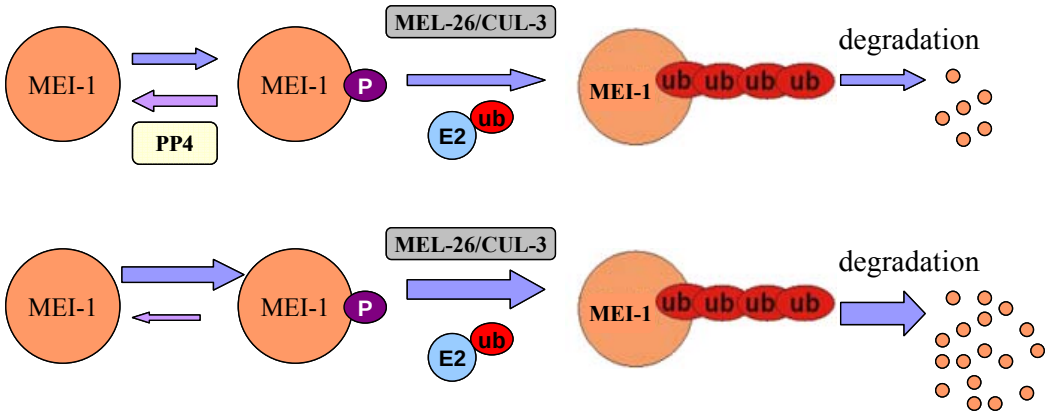

This model proposes that PP4 inhibits MEI-1 degradation. Eliminating PP4 would result in increased amount of phosphorylated MEI-1 to be degraded.

B. anti-MEI-1 staining of *mei-1(gf)* and *mei-1(gf); ppfr-1(RNAi)* embryos.

a) Percentages of MEI-1 positive early embryos were scored for each strain. The same result was seen when P. Mains scored the photos.

	anti-MEI-1(20°C)	Positive/total One- and two-cell	% Hatching (RNAi)
mei-1(gf)	Control	32/33	1.0
	mei-1(gf); pph-4.1(RNAi)	66/68	17.5
	mei-1(gf); ppfr-1(RNAi)	88/88	12.8
mel-26	Control	58/58	0.1
	mel-26; pph-4.1	58/58	8.4
	mel-26; ppfr-1(RNAi)	96/96	10.0

b) Examples of embryos with or without ectopic MEI-1

anti-MEI-1 **anti-α-tubulin**

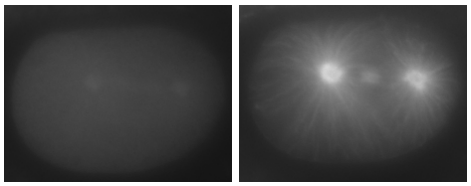

mei-1(ct46); pph-4.1
A one-cell embryo which is positive for ectopic MEI-1

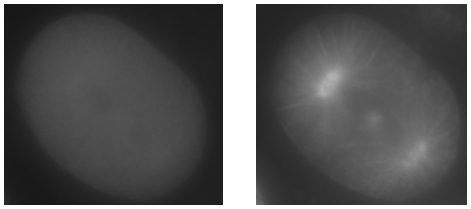

mei-1(ct46); pph-4.1
A one-cell embryo which is negative for ectopic MEI-1

Figure 7: Eliminating PP4 in *mel-26* mutants results in increase in the percentage of one-cell embryos with normal mitotic spindles.

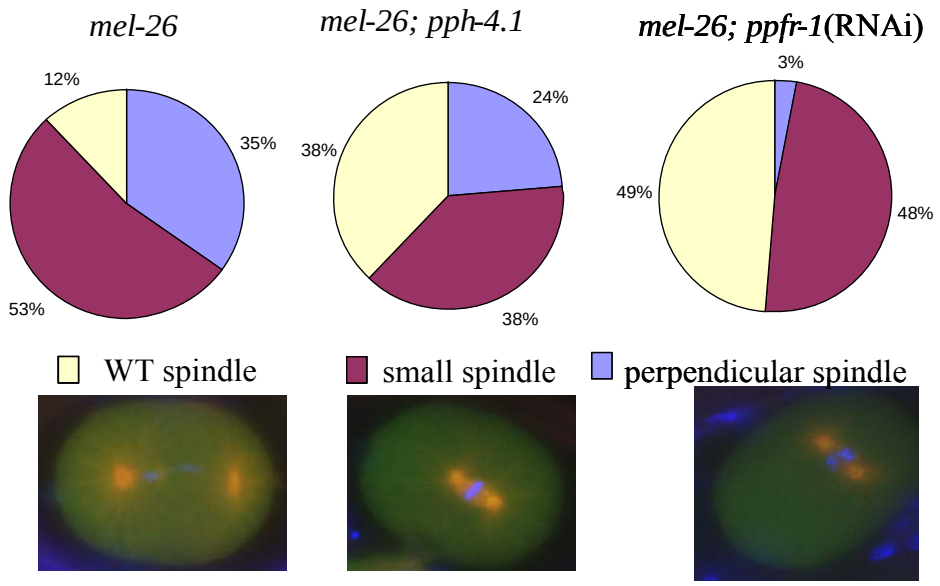

At 20°C, fixed one-cell embryos were divided into three groups based on spindle morphology: embryos with small and inclined spindles (blue, e.g., right embryo), embryos with small but properly orientated spindles (purple, e.g., centre embryo), and embryos with wild-type spindles (yellow, e.g., left embryo). When PP4 was inactivated by *ppfr-1* RNAi, the percentage of embryos with wild-type spindles increased from 12% to 49% at the expense of those with abnormal spindles.

Figure 8: Spindle orientation at 20°C.

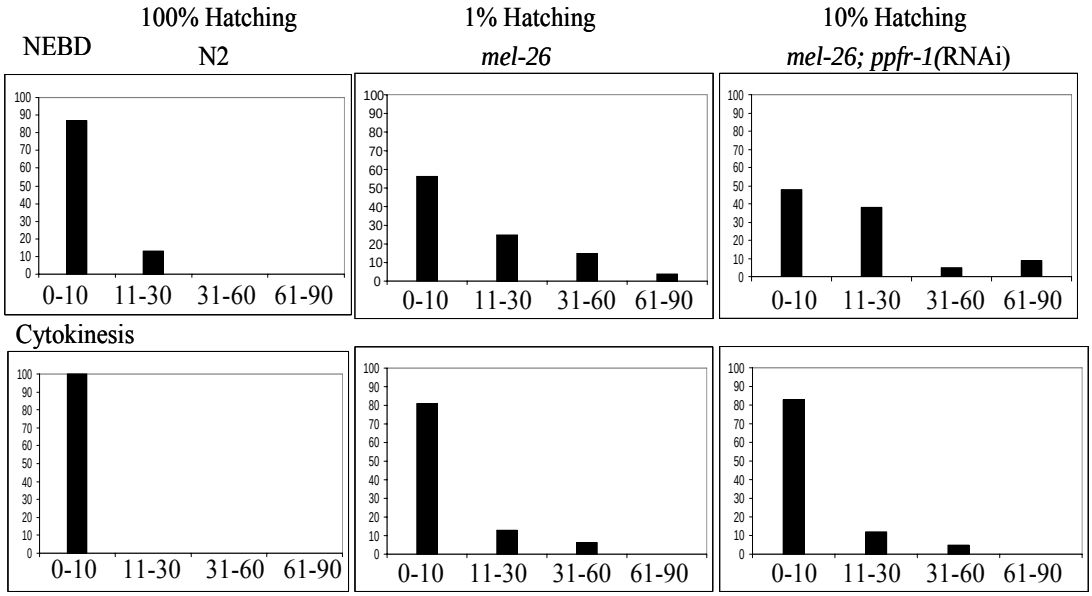

Y axis: percentage of total scored embryos in each category ($n \geq 23$).

X axis: spindle orientation. The scored embryos were divided into four groups based on the angles formed by line connecting two spindle poles and the A-P axis (Figure 4): normal (< 10°), slightly inclined (11° to 30°), moderately inclined (31° to 60°) and steeply inclined (61° to 90°).

Figure 9: The fractional spindle length at 20°C

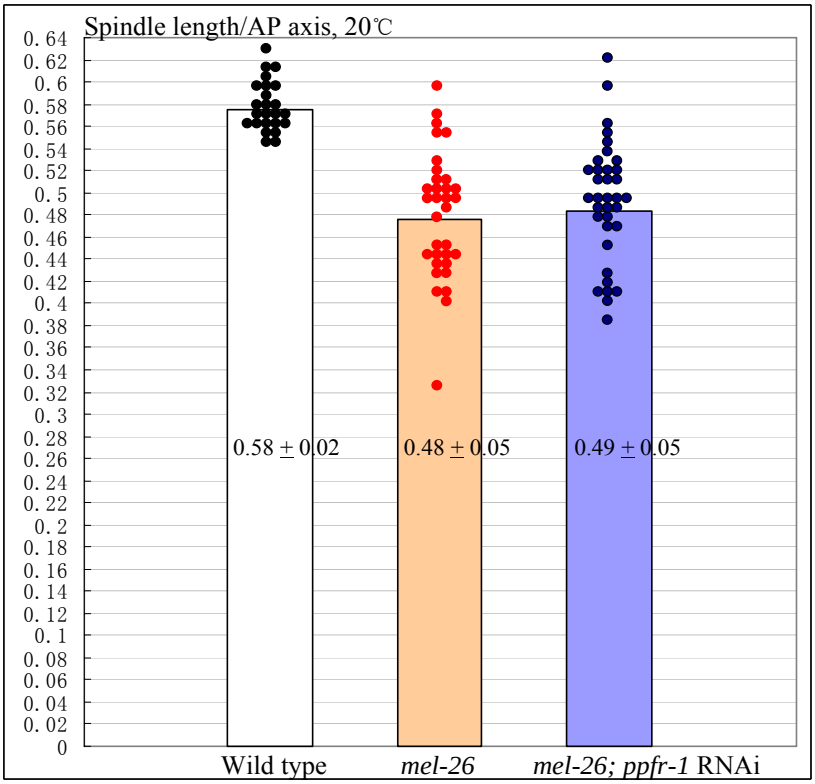

Y axis: ratio of the distance between spindle poles compared to length of A-P axis at cytokinesis. One dot represents one scored embryo.

Figure 10: Spindle orientation at 25°C.

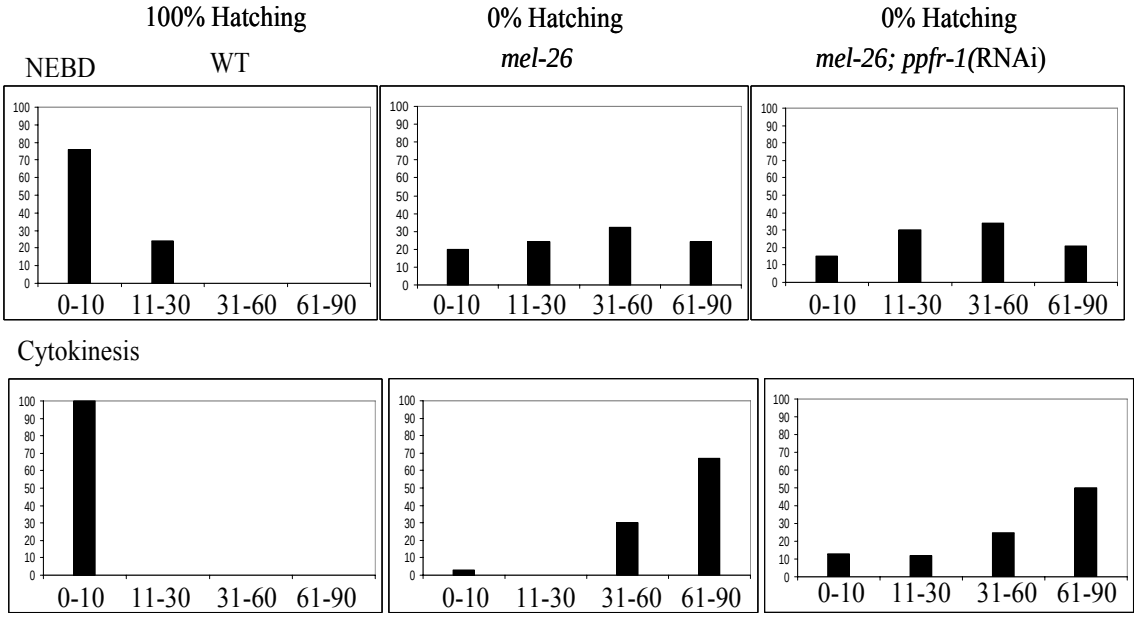

Y axis: percentage of total scored embryos ($n \geq 23$).

X axis: spindle orientation is defined the same as in Figure 8.

Figure 11: The fractional spindle length at 25°C

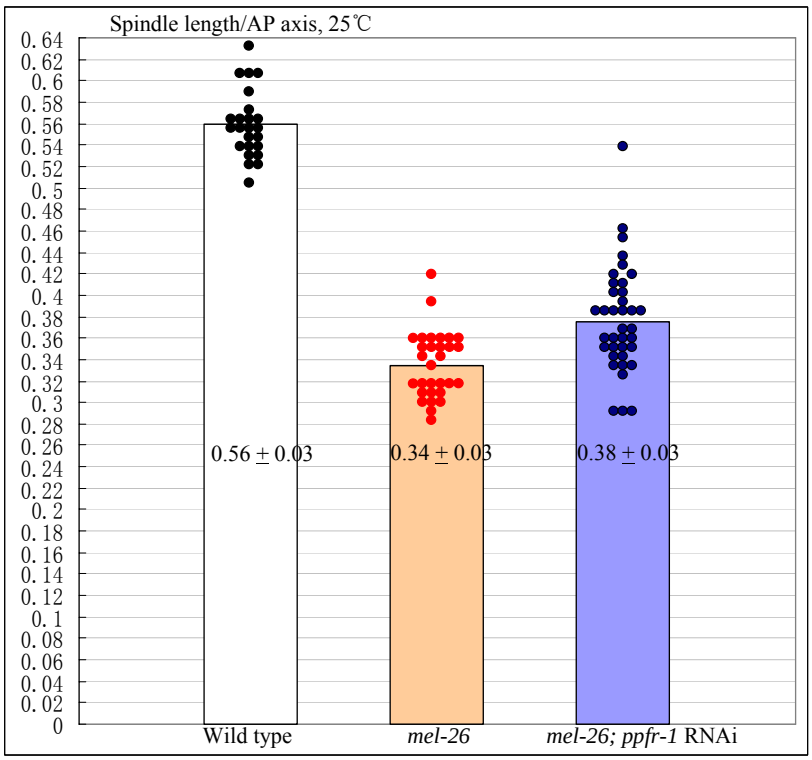

Y axis: ratio of the distance between spindle poles compared to length of A-P axis at cytokinesis. One dot represents one scored embryo.

Figure 12: Model Three: PP4 regulates MEI-1 activity.

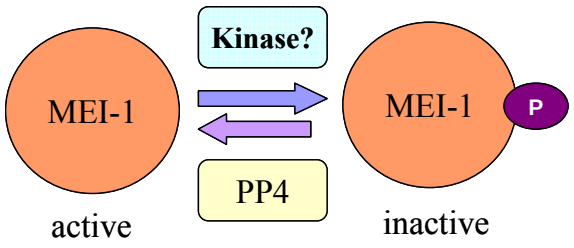

According to this model, PP4 counteracts an unknown kinase required to inactivate MEI-1 when meiosis was complete. Loss of PP4 would shift the balance so that ectopic MEI-1 was less active.

Figure 13: PPH-4.1 and MEI-1 may bind to each other.

A. PPH-4.1 and MEI-1 were co-purified with each other in reciprocal co-IP experiments

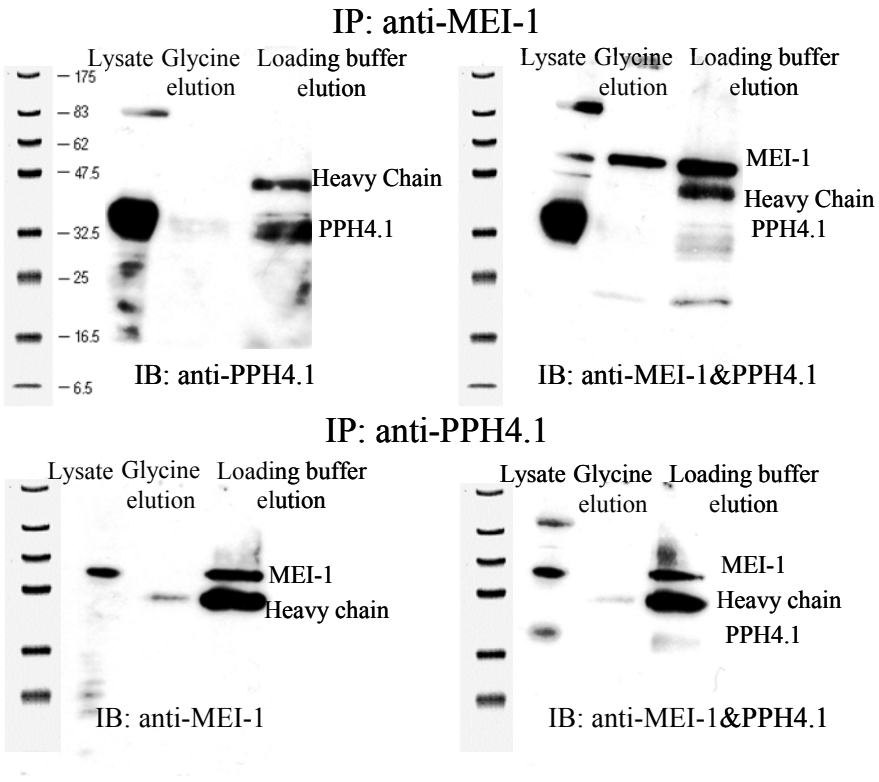

B. Neither PPH-4.1 nor MEI-1 was purified by mock IP with rabbit IgG

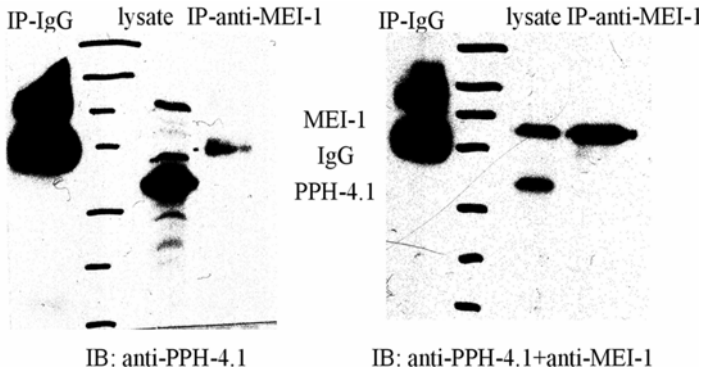

Chapter Four: Discussion and Future Directions

mei-1 encodes the worm "katanin" microtubule-severing protein. It is required during meiosis to regulate the shape and dynamics of meiotic spindles but must be degraded before mitosis (McNally *et al.*, 1993, Clark-Maguire and Mains 1994ab, Srayko *et al*., 2000, Srayko *et al*. 2006, McNally *et al.*, 2006). Degradation of post-meiotic MEI-1 is carried out by MEL-26/CUL-3 ubiquitin ligase (Dow and Mains, 1998, Furukawa *et al*, 2003, Pintard *et al*, 2003, Xu *et al*, 2003), MBK-2 kinase (Ming Pang *et al*, 2004, Quintin *et al.*, 2003, Pellettieri *et al.*, 2003, Stitzel *et al.*, 2006) as well as the cell cycle control component APC (Lu and Mains, 2007). My thesis focused on the major question of whether there are any other mechanisms to regulate MEI-1.

The regulatory subunit of PP4, *ppfr-1*, was identified as a suppressor of a *mei-1(gf)* allele in an RNAi screen by C. Birmingham. In my work, I found three PP4 subunits regulated post-meiotic MEI-1 in the same sense and PP4/MEI-1 interactions could be direct.

4.1 PP4 regulate MEI-1 during mitosis but not in meiosis.

It was shown that in *mei-1(gf),* eliminating PP4 suppressed embryonic lethality of post-meiotic MEI-1, suggesting a role of PP4 in regulating MEI-1 when it ectopically persists into mitosis. To address whether PP4 also regulates MEI-1 during meiosis, C. Birmingham did *ppfr-1(RNAi)* to a weak *lf* mutant of *mei-2* with partially compromised MEI-1 activity during meiosis. If PP4(+) is also a positive regulator of meiotic MEI-1 activity, then knocking down PP4 should have increased the lethality of the hypomorphic *mei-2(lf)* allele. However, no interaction was observed between *ppfr-1* and *mei-2* (Table 1), indicating regulation of MEI-1 by PP4 is restricted to the post-meiotic divisions.

Consistent with this finding, RNAi experiments showed that *pph-4.1* is dispensable for female meiotic divisions of fertilized eggs (Sumiyoshi *et al.*, 2002). Although it may play a role in recombination, no PP4 protein was detected in the meiotic spindles by immunochemical staining with antibody against PPH-4.1 (Sumiyoshi *et al.*, 2002).

4.2 Catalytic vs. Regulatory subunits of PP4.

Previously it was shown that mammalian R1or R2 regulatory subunits might inhibit activity of the catalytic subunit PP4c *in vitro* (Hastie *et al.*, 2000, Kloeker and Wadzinski, 1999). In contrast to their findings, my work demonstrated that the PPFR-1/PP4R1 regulatory subunit acts in concert with PPH-4.1/PP4c catalytic subunit in *C. elegans* (Table 3A). A possible explanation for the above discrepancy, as pointed out by the authors (Hastie *et al.*, 2000, Kloeker and Wadzinski, 1999), is that the regulatory subunit endows the catalytic subunits with substrate specificity. In the reported assays, casein and phosphorylase were used as the substrate, but these are unlikely to be physiologically relevant. Thus PP4 regulatory subunits could inhibit activity of catalytic subunit against substrates like casein and phosphorylase, which were used in the *in vitro* studies, but they increase PP4c activity with the true physiological substrates.

Loss of distinct PP4 subunits causes different extents of embryonic lethality. For example, complete loss of PPH-4.1 or PPFR-3 results in almost 100% lethality, while removing the PPFR-1/R1 regulatory subunit (as shown for the deletion mutant, which is a likely null) just results in moderate lethality of 15% (Table 3B and Table 4). This suggests although the PP4 phosphatase holoenzyme involved in MEI-1 regulation may be composed of PPH-4.1, PPFR-1 and PPFR-3, other forms of PP4, lacking PPFR-1, must also exist in *C. elegans* and function in essential processes, which were not investigated

in my studies. For example, in both *Drosophila* and *C. elegans*, reduction of PP4c/PPH-4.1 protein level alters mitotic spindle assembly and also recruitment of centrosome components, such as γ-tubulin (Helps *et al.*, 1998, Sumiyoshi *et al.*, 2002).

Since simultaneous RNAi against both *pph-4.1* and *ppfr-1* showed the same rescuing capacity as either alone (Table 3), it is possible that depletion of the PPFR-1 regulatory subunit rescues lethality via regulating localization of the PPH-4.1 catalytic subunit. I attempted to see if knocking down the *ppfr-1* regulatory subunit would affect PPH-4.1 localization. Unfortunately after shipment, Dr. Sugimoto's anti-PPH-4.1 no longer detected PPH-4.1 by immunolocalization, although it is still effective on western blots and for IP. We asked if we could collaborate by testing this possibility in her laboratory, but the person who did the PPH-4.1 immunolocalization studies has left her lab.

4.3 Where does PP4 fit in MEI-1 degradation/ inactivation pathways?

PP4 RNAi suppresses ectopic MEI-1 in *mel-26(null)*, suggesting it is involved in a pathway parallel to *mel-26*. If the genes acted sequentially, knocking down PP4 when *mel-26* was completely gone would have had no effect. Since MBK-2 and APC eliminate MEI-1 redundantly with MEL-26 at lower temperatures (15°C and 20°C), it is possible that PP4 is involved in the MBK-2 or APC pathways to regulate MEI-1 degradation. My results do not favor the model that PP4 counteracts *mbk-2*. First, at 20°C PP4 RNAi did not rescue an *mbk-2(ts)* partial loss of function mutant (Table 6A). If PP4 counteracts MBK-2, reducing the phosphatase would shift MEI-1 to the phosphorylated form, thus lethality caused by partial loss of MBK-2 kinase might have been suppressed. My observations do not support this possibility, although it might have been difficult to detect

because MBK-2 has other essential targets besides MEI-1 (Stitzel *et al.*, 2006). Second, I have shown that at 25°C the morphology of the first mitotic spindles became better by knocking down PP4 in *mei-1(gf)*. If this change in spindle morphology is a result of shift of the balance of MEI-1 modifications, namely a net increase in the phosphorylation of MEI-1 relative to the *mbk-2* mutant alone, this difference in MEI-1 phosphorylation should have been observed by immunochemical staining with anti-Phospho-MEI-1 (Stitzel *et al.*, 2006). However, results were negative, although subtle difference may exist (Table 6B). Taken together, it seems PP4 is involved in a pathway parallel to MEL-26 and it does not counteract MBK-2.

4.4 PP4 regulates MEI-1 degradation or activity.

Although PP4 does not appear to act in concert with MBK-2 to regulate MEI-1 degradation, it could affect MEI-1 turnover (or perhaps localization) through other pathways. At 20°C eliminating PP4 increased the hatching rate but not the percentage of MEI-1 negative embryos in *mei-1(gf)*. Furthermore, there was no obvious change in protein level in the positive embryos or localization pattern of ectopic MEI-1 based on anti-MEI-1 immunochemical staining or western blots. It is possible that subtle changes in protein levels may not have been detected yet were still sufficient to increase the hatching rate, but this possibly is unlikely in view of the finding that the percentage of MEI-1 negative embryos closely correlated with hatching rates in all genetic backgrounds scored by Lu and Mains (Lu and Mains, 2007). Thus I proposed PP4 is involved in regulating MEI-1 activity rather than protein degradation or localization.

An *in vitro* glass immobilized assay has been reported as the most reliable and rapid assay for MT severing activity (McNally *et al.*, 2006). In this assay, bacterially-

expressed worm MEI-1-MEI-2 complex was purified and added to rhodamine labelled, taxol-stabilized MTs and severing activity was calculated by the increase of MT fragments. To investigate the role of PP4 in regulating katanin activity, worm embryo extracts from *mei-1(gf)* and *mei-1(gf) ppfr-1* could be scored for MT-severing activity by the above assay. If katanin mediated MT-severing is reduced in extract of the latter, this would suggest that PP4 is required to maintain MEI-1 activity and loss of PP4 reduces MEI-1 enzymatic activity.

4.5 Does PP4 bind to MEI-1?

By reciprocal co-IP experiments, I have shown that PP4 directly bound to MEI-1. This finding is promising but results were not consistently repeatable. The inconsistency could have been due to transient or unstable binding between PPH-4.1 and MEI-1. I am confident that the co-immunoprecipitated bands were indeed MEI-1 and PPH-4.1 since they were at the appropriate molecular weights and proteins of those sizes were not immunoprecipitated by rabbit IgG (Figure 13B) or a control antibody, anti-CBLB (data not shown). In addition, a band at the MEI-1 molecular weight was not seen when westerns were probed with anti-PPH-4.1 after anti-PPH-4.1 immunoprecipitation and *vice versa*. Thus, I saw the appropriate bands in 5 of 10 experiments but in 0 of 4 controls.

The possibility of low total protein abundance resulting in the inconsistent results is ruled out for two reasons. First, I showed that both PPH-4.1 and MEI-1 proteins are of moderate abundance in worm lysate since each was always readily detected when western blots were probed with the same antibody used for immunoprecipiation. Second, results were also negative with 10 fold increase in input lysate, suggesting protein

abundance is not the limiting factor of this experiment. Chemical crosslinkers have been applied to fix transient interactions (Melcher 2004). By using bifunctional reagents with reactive end groups against functional groups of amino acid residues, covalent bonds will form between two proteins. Specifically, when reversible homo-bifunctional crosslinkers such as N-hydroxysuccinimide (NHS) esters are used, interacting proteins can be recovered by treatment with thiols, such as β–mercaptoethanol or dithiothreitol. This technique could facilitate confirmation of my inconsistent co-IP results.

Another technique to provide convincing evidence for protein interactions would be Y2H assays. However, this technique has the caveat that yeast might lack the phosphorylation pathway, which could be the prerequisite of the stable PP4-MEI-1 interaction. To overcome this, it would be better to pursue the identity of the kinase that acts antagonistically with PP4, which will be discussed in the following section.

4.6 An unknown kinase – a new *mei-1* pathway component.

My results favour a model that PP4 counteracts an unknown kinase to regulate MEI-1 activity. Since the interaction between PP4 and MEI-1 is transient or weak based on my co-IP results, it may be easier to carry out further studies with the corresponding kinase, which could be potentially found by RNAi screening.

In the *C. elegans* genome, 470 genes are predicted kinases (www.wormbase.org). RNAi against the PP4 counteracting kinase should enhance the remaining lethality caused by ectopic MEI-1 in *mei-1(gf) ppfr-1*, that is, it would block the rescue of *mei-1(gf)* by *ppfr-1*. If this kinase is also involved in an essential process, knocking down the kinase in wild type may result in unrelated high embryonic lethality. In this case conditional RNAi should be performed by reducing the feeding time of worms on dsRNA

producing bacteria. Once the kinase was identified, its role on *mei-1* regulation could be characterized. For example, by analyzing interactions between this kinase and *mei-1(lf)*, we will see if it also regulates MEI-1 during meiosis. With antisera generated against this kinase, expression pattern could be analyzed. Presumably it also localizes to the spindle poles. We could also find the corresponding phosphorylation site and perhaps by *in vitro* studies we will be able to show MEI-1 is phosphorylated by this kinase and dephosphorylated by PP4.

To summarize, I have examined the role of PP4 in regulating post-meiotic MEI-1. Although the exact mechanism of PP4 regulation of MEI-1 remains unclear, my work reflects another system to ensure the accurate control of MEI-1 besides the major degradation pathways.

References

Albertson DG. (1984). Formation of the first cleavage spindle in nematode embryos. *Dev Biol.* **101**, 61-72.

Aldaz H, Rice LM, Stearns T, Agard DA. (2005) Insights into microtubule nucleation from the crystal structure of human gamma-tubulin. *Nature* **435,** 523-7.

Allen C, Borisy GG. (1974) Structural polarity and directional growth of microtubules of Chlamydomonas flagella. *J Mol Biol.* **90**, 381-402.

Amos L, Klug A. (1974). Arrangement of subunits in flagellar microtubules. *J Cell Sci.* **14**, 523-49.

Brenner S. (1974). The genetics of *Caenorhabditis elegans*. *Genetics* **77**, 71-94.

Brewis ND, Street AJ, Prescott AR, Cohen PT. (1993) PPX, a novel protein serine/threonine phosphatase localized to centrosomes. *EMBO J.* **12**, 987-96.

Chalfie M, Thomson JN. (1982) Structural and functional diversity in the neuronal microtubules of *Caenorhabditis elegans*. *J Cell Biol.* **93**, 15-23.

Chen J, Peterson RT, Schreiber SL. (1998) Alpha 4 associates with protein phosphatases 2A, 4, and 6. *Biochem Biophys Res Commun*. **247**, 827-32.

Clandinin TR, Mains PE. (1993) Genetic studies of *mei-1* gene activity during the transition from meiosis to mitosis in *Caenorhabditis elegans*. *Genetics* **134**, 199-210.

Clark-Maguire S, Mains PE. (1994a) *mei-1*, a Gene Required for Meiotic Spindle Formation in *Caenorhabditis elegans*, Is a Member of a Family of ATPases. *Genetics* **136**, 533-46.

Clark-Maguire S, Mains PE. (1994b) Localization of the *mei-1* gene product of *Caenorhaditis elegans*, a meiotic-specific spindle component. *J. Cell Biol.* **126**, 199-209.

Cohen PT, Philp A, Vazquez-Martin C. (2005) Protein phosphatase 4--from obscurity to vital functions. *FEBS Lett*. **579**, 3278-86.

Dow MR, Mains PE. (1998) Genetic and molecular characterization of the *Caenorhabditis elegans* gene, *mel-26*, a postmeiotic negative regulator of *mei-1*, a meiotic-specific spindle component. *Genetics* **150**, 119-28.

Fire A, Xu S, Montgomery MK, Kostas SA, Driver SE, Mello CC. (1998) Potent and specific genetic interference by double-stranded RNA in *Caenorhabditis elegans*. *Nature* **391**, 806-11.

Furukawa M, He YJ, Borchers C, Xiong Y. (2003) Targeting of protein ubiquitination by BTB-Cullin 3-Roc1 ubiquitin ligases. *Nat Cell Biol*. **5**, 1001-7.

Gengyo-Ando K, Mitani S. (2000) Characterization of mutations induced by ethyl methanesulfonate, UV, and trimethylpsoralen in the nematode *Caenorhabditis elegans*. *Biochem Biophys Res Commun*. **269**, 64-9.

Gomes JE, Encalada SE, Swan KA, Shelton CA, Carter JC, Bowerman B. (2001) The maternal gene spn-4 encodes a predicted RRM protein required for mitotic spindle orientation and cell fate patterning in early C. elegans embryos. *Development* **128**, 4301-14

Hartman JJ, Mahr J, McNally K, Okawa K, Iwamatsu A, Thomas S, Cheesman S, Heuser J, Vale RD, McNally FJ. (1998) Katanin, a microtubule-severing protein, is a novel AAA ATPase that targets to the centrosome using a WD40-containing subunit. *Cell* **93**, 277-87.

Hastie CJ, Carnegie GK, Morrice N, Cohen PT. (2000) A novel 50 kDa protein forms complexes with protein phosphatase 4 and is located at centrosomal microtubule organizing centres. *Biochem J*. **347**, 845-55.

Heald R, Walczak CE. (1999) Microtubule-based motor function in mitosis. *Curr Opin Struct Biol.* **9**, 268-74.

Helps NR, Brewis ND, Lineruth K, Davis T, Kaiser K, Cohen PT. (1998) Protein phosphatase 4 is an essential enzyme required for organisation of microtubules at centrosomes in *Drosophila* embryos. *J Cell Sci.***111**, 1331-40.

Hyman AA, White JG. (1987) Determination of cell division axes in the early embryogenesis of *Caenorhabditis elegans. J. Cell Biol.* **105,** 2123–2135.

Inui S, Kuwahara K, Mizutani J, Maeda K, Kawai T, Nakayasu H, Sakaguchi N. (1995) Molecular cloning of a cDNA clone encoding a phosphoprotein component related to the Ig receptor-mediated signal transduction. *J Immunol*. 154**, 2714-23.**

Kamath RS, Ahringer J. (2003) Genome-wide RNAi screening in *Caenorhabditis elegans*. *Methods* **30**, 313-21.

Kemphues KJ, Wolf N, Wood WB, Hirsh D. (1986) Two loci required for cytoplasmic organization in early embryos of *Caenorhabditis elegans*. *Dev Biol.* **113**, 449-60.

Kloeker S, Wadzinski BE. (1999) Purification and identification of a novel subunit of protein serine/threonine phosphatase 4. *J Biol Chem*. **274**, 5339-47.

Kuwahara K, Matsuo T, Nomura J, Igarashi H, Kimoto M, Inui S, Sakaguchi N. (1994) Identification of a 52-kDa molecule (p52) coprecipitated with the Ig receptor-related MB-1 protein that is inducibly phosphorylated by the stimulation with phorbol myristate acetate. *J Immunol*. **152**, 2742-52.

Li S, Armstrong CM, Bertin N, Ge H, Milstein S, Boxem M, Vidalain PO, Han JD, Chesneau A, Hao T, Goldberg DS, Li N, Martinez M, Rual JF, Lamesch P, Xu L, Tewari M, Wong SL, Zhang LV, Berriz GF, Jacotot L, Vaglio P, Reboul J, Hirozane-Kishikawa T, Li Q, Gabel HW, Elewa A, Baumgartner B, Rose DJ, Yu H, Bosak S, Sequerra R, Fraser A, Mango SE, Saxton WM, Strome S, Van Den Heuvel S, Piano F, Vandenhaute J, Sardet C, Gerstein M, Doucette-Stamm L, Gunsalus KC, Harper JW, Cusick ME, Roth FP, Hill DE, Vidal M. (2004) A map of the interactome network of the metazoan *C. elegans*. *Science* **303**, 540-3.

Lu C, Mains PE. (2005) Mutations of a redundant alpha-tubulin gene affect *Caenorhabditis elegans* early embryonic cleavage via MEI-1/katanin-dependent and -independent pathways. *Genetics* **170**, 115-26.

Lu C, Mains PE. (2007) The *C. elegans* anaphase promoting complex and MBK-2/DYRK kinase act redundantly with CUL-3/MEL-26 ubiquitin ligase to degrade MEI-1 microtubule-severing activity after meiosis. *Dev Biol*. **302**, 438-47.

Mains PE, Kemphues KJ, Sprunger SA, Sulston IA, Wood WB. (1990b) Mutations affecting the meiotic and mitotic divisions of the early *Caenorhabditis elegans* embryo. *Genetics* **126**, 593-605.

Mains PE, Sulston IA, Wood WB. (1990a) Dominant maternal-effect mutations causing embryonic lethality in *Caenorhabditis elegans*. *Genetics* **125**, 351-69.

Matthews LR, Carter P, Thierry-Mieg D, Kemphues K. (1998) ZYG-9, a *Caenorhabditis elegans* protein required for microtubule organization and function, is a component of meiotic and mitotic spindle poles. *J Cell Biol.* **141**, 1159-68.

McCarter J, Bartlett B, Dang T, Schedl T. (1999) On the control of oocyte meiotic maturation and ovulation in *Caenorhabditis elegans*. *Dev Biol.* **205**, 111-28.

McNally K, Audhya A, Oegema K, McNally FJ. (2006) Katanin controls mitotic and meiotic spindle length. *J Cell Biol*. **175**, 881-91

McNally FJ, Vale RD. (1993) Identification of katanin, an ATPase that severs and disassembles stable microtubules. *Cell* **75**, 419-29

Melcher K. (2004) New chemical crosslinking methods for the identification of transient protein-protein interactions with multiprotein complexes. *Curr Protein Pept Sci*. **5**: 287-96.

Miller DM, Shakes DC. (1995) Immunofluorescence microscopy. *Methods Cell Biol.* 48: 365-94.

Ming Pang K, Ishidate T, Nakamura K, Shirayama M, Trzepacz C, Schubert CM, Priess JR, Mello CC. (2004) The minibrain kinase homolog, *mbk-2*, is required for spindle positioning and asymmetric cell division in early *C. elegans* embryos. *Dev. Biol.* **265**, 127-139.

Nanahoshi M, Tsujishita Y, Tokunaga C, Inui S, Sakaguchi N, Hara K, Yonezawa K. (1999) Alpha4 protein as a common regulator of type 2A-related serine/threonine protein phosphatases. *FEBS Lett.* **446**, 108-12.

Patel N, Thierry-Mieg D, Mancillas JR. (1993) Cloning by insertional mutagenesis of a cDNA encoding *Caenorhabditis elegans* kinesin heavy chain. *Proc Natl Acad Sci U S A.* **90**, 9181-5.

Pellettieri J, Reinke V, Kim SK, Seydoux G. (2003) Coordinate Activation of Maternal Protein Degradation during the Egg-to-Embryo Transition in *C. elegans*. *Dev. Cell* **5**, 451-62.

Phillips JB, Lyczak R, Ellis GC, Bowerman B.(2004) Roles for two partially redundant alpha-tubulins during mitosis in early *Caenorhabditis elegans* embryos. *Cell Motil Cytoskeleton* **58**, 112-26.

Pintard L, Willis JH, Willems A, Johnson JL, Srayko M, Kurz T, Glaser S, Mains PE, Tyers M, Bowerman B, Peter M. (2003) The BTB protein MEL-26 is a substrate-specific adaptor of the CUL-3 ubiquitin-ligase. *Nature* **425**, 311-6.

Quintin S, Mains PE, Zinke A, Hyman AA. (2003) The *mbk-2* kinase is required for inactivation of MEI-1/katanin in the one-cell *Caenorhabditis elegans* embryo. *EMBO Rep* **4**, 1175-1181.

Rechsteiner M, Rogers SW. (1996) PEST sequences and regulation by proteolysis. *Trends Biochem Sci.* **21**, 267-71

Rogers S, Wells R, Rechsteiner M. (1986) Amino acid sequences common to rapidly degraded proteins: the PEST hypothesis. *Science* **234**, 364-8.

Schatten G. (1994). The centrosome and its mode of inheritance: the reduction of the centrosome during gametogenesis and its restoration during fertilization. *Developmental Biology* **165,** 299-335.

Srayko M, Mains PE. (2000) MEI-1/MEI-2 katanin-like microtubule severing activity is required for *Caenorhabditis elegans* meiosis. *Genes & Development* **14**, 1072–1084.

Srayko M, O'toole ET, Hyman AA, Muller-Reichert T. (2006) Katanin disrupts the microtubule lattice and increases polymer number in *C. elegans* meiosis. *Curr Biol.* **16**, 1944-9.

Stitzel ML, Pellettieri J, Seydoux G. (2006) The *C. elegans* DYRK Kinase MBK-2 Marks Oocyte Proteins for Degradation in Response to Meiotic Maturation. *Curr Biol*. **16**, 56-62.

Sumiyoshi E, Sugimoto A, Yamamoto M. (2002) Protein phosphatase 4 is required for centrosome maturation in mitosis and sperm meiosis in *C. elegans*. *J. Cell Sci.* **115**, 1403-10.

Strome S, Wood WB. (1983) Generation of asymmetry and segregation of germ-line granules in early *C. elegans* embryos. *Cell* **35**, 15–25.

Sulston JE, Schierenberg E, White JG, Thomson JN. (1983) The embryonic cell lineage of the nematode *Caenorhabditis elegans*. *Dev Biol*. **100**, 64-119.

Tabara H, Grishok A, Mello CC. (1998) RNAi in C. elegans: soaking in the genome sequence. *Science* **282**, 430-1.

Tavernarakis N, Wang SL, Dorovkov M, Ryazanov A, Driscoll M. (2000) Heritable and inducible genetic interference by double-stranded RNA encoded by transgenes. *Nat Genet.* **24**, 180-3

Timmons L, Court DL, Fire A. (2001) Ingestion of bacterially expressed dsRNAs can produce specific and potent genetic interference in Caenorhabditis elegans. *Gene* **263**, 103-12.

van der Wijk T, Blanchetot C, den Hertog J. (2005) Regulation of receptor protein-tyrosine phosphatase dimerization. *Methods* **35**, 73-9.

Wada T, Miyata T, Inagi R, Nangaku M, Wagatsuma M, Suzuki D, Wadzinski BE, Okubo K, Kurokawa K. (2001) Cloning and characterization of a novel subunit of protein serine/threonine phosphatase 4 from mesangial cells. *J Am Soc Nephrol* **12**, 2601-8.

Winston JT, Strack P, Beer-Romero P, Chu CY, Elledge SJ, Harper JW. (1999) The SCFbeta-TRCP-ubiquitin ligase complex associates specifically with phosphorylated destruction motifs in IkappaBalpha and beta-catenin and stimulates IkappaBalpha ubiquitination in vitro. *Genes Dev*. **13**, 270-83. Erratum in: *Genes Dev.* **13**, 1050.

Xu L, Wei Y, Reboul J, Vaglio P, Shin TH, Vidal M, Elledge SJ, Harper JW. (2003) BTB proteins are substrate-specific adaptors in an SCF-like modular ubiquitin ligase containing CUL-3. *Nature* **425**, 316-21.

Yang HY, Mains PE, McNally FJ. (2005) Kinesin-1 mediates translocation of the meiotic spindle to the oocyte cortex through KCA-1, a novel cargo adapter. *J Cell Biol*. **169**, 447-57.